DOE/MC/21181-1950, Vol 13
(DE89011674)
Distribution Category UC-132

Geological Evolution and Analysis of Confirmed or Suspected Gas Hydrate Localities

Volume 13. Basin Analysis, Formation and Stability of Gas Hydrates of the Nankai Trough

Topical Report

M. Ciesnik
J. Krason

Work Performed Under Contract No.: DE-AC21-84MC21181

For
U.S. Department of Energy
Office of Fossil Energy
Morgantown Energy Technology Center
P.O. Box 880
Morgantown, West Virginia 26507-0880

By
Geoexplorers International, Inc.
5701 East Evans Avenue
Denver, Colorado 80222

May 1989

CONTENTS

Page

FIGURES

TABLES

BASIN ANALYSIS, FORMATION AND STABILITY OF GAS HYDRATES OF THE NANKAI TROUGH

by

Mark Ciesnik and Jan Krason

EXECUTIVE SUMMARY

Geological factors controlling the formation, stability, and distribution of gas hydrates were investigated by basin analysis of the Nankai Trough region. Geological, geophysical, and geochemical data from the region were assembled and critically evaluated to develop consistent interpretations of the relationships of geological environments and gas hydrates.

This study was performed for the U.S. Department of energy Morgantown Energy Technology Center by Geoexplorers International, Inc. as part of a worldwide evaluation of 21 offshore sites where the presence of gas hydrates has been confirmed or inferred.

The Nankai Trough is located beneath the western Pacific, south of the Japanese islands Shikoku and central Kyushu. The trough strikes in a northeast-southwest direction. The southern flank of the central and western trough displays a smooth transition into the abyssal plain of the Shikoku Basin. The eastern limit of the study region is the Zenisu ridge. The Kyushu-Palau ridge constitutes the western limit of the Nankai Trough. The eastern area of the trough ends in the vicinity of the Nishishichto Ridge which strikes north to south. This ridge is also known as Izu-Bonin Ridge. The entire area as outlined above is approximately 450 km long with the width varying from 20 to 60 km.

Nankai Trough jointly with the landward slope constitute the continental margin of southwest Japan. This continental margin includes the areas east of Kyushu, south of Shikoku, and the Kii peninsula of the Honshu island (Nankai), as well as east of the Kii peninsula. A narrow continental shelf is found offshore of southwest Japan. Periodic seismic uplifts of coastal promontories, in conjunction with the subsidence of the sea floor, have resulted in deep embayments of the shoreline. Two geomorphologically distinct sections of the continental slope are easily discernible in the area adjacent to the Nankai Trough. The upper and lower slope sections are separated by a discontinuous series of flat-surfaced terraces. The terraces occur at a sea depth between 200 and 1,200 m. The upper slope section has a mostly uniform and only a slightly geomorphologically differentiated surface, but

the lower slope displays a more diverse relief. The most noticeable feature of the lower landward slope area along the Nankai Trough is the presence of a series of ridges parallel to the trough. The ridges emerge along thrusts rooted in the basal detachment beneath the slope, and thus appear to be structurally controlled.

Tectonically the Nankai Trough is part of a complex area of active margins marked by a well developed system of trenches. Although its western and eastern limits are delineated by ridges, the Nankai Trough continues to the southwest as Ryuku trench. In an eastern direction it merges at the triple junction with the Japan trench from the north and the Mariana-Izu trench from the south. The system of trenches mentioned above, south and east of the Japan islands, separates three major tectonic plates in the region, the Pacific plate, the Eurasia plate, and the Philippine plate.

Two principal types of sedimentation have been discerned on the basis of lithological profiles, both in deformed and undeformed sediments of the Nankai Trough. The turbidite sequences, represented by interbedded sandstone and shale with turbidite sedimentary structures, appear to form the upper 500 m of the sedimentary profile. The lower sedimentary unit consists predominantly of hemipelagic muds.

Adequate organic carbon for bacterial methanogenesis exists in the few drilled holes on the continental slope of the Nankai Trough study region. Sediments within the gas hydrate stability zone are immature with respect to thermogenic methane formation.

Seismic recordings from the Nankai Trough in the public domain feature BSRs most likely related to gas hydrates. Migrated seismic lines 54K-1-2, 55N-1, and 55N-3-1 obtained by Japan Petroleum Exploration from the ship Kaiyo Maru show very well developed BSRs. Despite the fact that structural features are obscure in many sections, distinct and mostly continuous BSRs occur in lower sections of the continental slope.

Based on areal extent of BSRs potential gas resources contained in gas hydrates were estimated at between 10^{11} m^3 (4 TCF) and 10^{13} m^3 (400 TCF) depending on the thickness assumed for the gas hydrate bound sediment layer causing the BSR.

INTRODUCTION

Gas hydrates are solid substances composed of small gas molecules enclosed in a crystal lattice of water molecules. Gas hydrates can be formed from various gases and water at high pressures and low temperatures when a sufficiently high concentration of dissolved gas exists. Conditions favorable for natural gas hydrate formation and preservation occur in some continental margin and deep sea sediments where adequate amounts of hydrocarbon gases are available. Large quantities of natural gas with possible resource potential may be present in offshore gas hydrates or trapped beneath impermeable gas hydrate layers.

This report presents the results of a study on the geological factors which control the formation and stability of gas hydrates in the sediments of the Nankai Trough. The Nankai Trough study region comprises the Nankai Trough, the continental slope between the trough and Japan, and surrounding areas.. This study is part of a project performed for the U.S. Department of Energy's Morgantown Energy Technology Center by Geoexplorers International, Inc. The main purpose of the project is to evaluate the geological controls of gas hydrate formation and stability and to make preliminary assessments of gas resources associated with gas hydrates.

Migrated seismic sections from the Nankai Trough display very pronounced bottom simulating reflectors (BSRs). Bottom simulating reflectors are commonly accepted as indicators of gas hydrate presence in sediments. Bottom simulating reflectors occur extensively over an approximate area of 3.5×10^{10} m^2 in the Nankai Trough study region. Structurally this area coincides with the middle and upper continental slope. In the area of BSR occurrence, there is presently a shortage of geological data, as the only drilling activities have been carried out in the lowermost continental slope adjacent to the Nankai Trough (DSDP Sites 297, 298, 582, 583). Structural controls of the area are progressively less known in the upslope direction. We have applied data from these DSDP drilling sites in an examination of the gas hydrate potential in the context of major geological factors. Among these factors hydrocarbon generation potential and geothermal gradients may influence gas hydrate distribution in the Nankai Trough study region.

Analyses of hydrocarbon gases in sediments at DSDP Sites 298 and 583 conclusively showed their biogenic provenance. We suggest that production of the marine organic matter is the greatest in the middle and upper continental slope. Consequently, the potential for biogenically derived methane is greater there compared with lower sectors of the continental slope.

Given the set of assumptions for the area with presumed gas hydrate occurrence, we estimated methane resources in the gas hydrate zone of the Nankai Trough.

This report is presented in two sections:

Part I - Basin Analysis examines the structural geology and sedimentary environ-environments of the Nankai Trough study region. Based on this information, the regional hydrocarbon generation potential is discussed.

Part II - Formation and Stability of Gas Hydrates describes the seismic and drilling evidence of gas hydrate presence in the study region. The evidence is analyzed in detail in view of the information presented in Part I to indicate which factors may control the formation and stability of gas hydrates in the Nankai Trough study region.

Acknowledgements

Geoexplorers International, Inc. and the authors are grateful to the U.S. Department of Energy, Morgantown Energy Technology Center for the opportunity to participate in the gas hydrate research program. Rodney Malone of METC reviewed the report for technical content and style. Charles Komar expedited printing of this report.

PART I

BASIN ANALYSIS

The Nankai Trench study region is located offshore of the Pacific coasts of the Japanese islands of Shikoku and Kyushu. The present topography of the continental slope of the Nankai Trough study region is characterized by plateaus separated by steeper steps. These plateaus resulted from sediment ponding behind dams created by imbricate thrust sheets. The structure of the Nankai Trough study region is similar to other convergent margins, with an accretionary prism with imbricate thrusting with a broad forearc basin immediately landward. Hemipelagic sedimentation and frequent turbidite deposition are dominant sedimentary processes on both the trough itself and the continental slope. Adequate organic carbon for bacterial methanogenesis exists in the few drilled holes on the continental slope of the Nankai Trough study region. Sediments within the gas hydrate stability zone are immature with respect to thermogenic methane formation.

Location

The Nankai Trough is located beneath the western Pacific, south of the Japanese islands Shikoku and central Kyushu. The trough strikes in a northeast-southwest direction. A trough is defined as "an elongate depression of the sea floor that is wider and shallower than a trench, with less steeply dipping sides" (Bates and Jackson, 1980). Bottom simulating reflectors which indicate the presence of gas hydrates have been reported on seismic lines from the Nankai Trough (Aoki et al., 1982, Kvenvolden and Barnard, 1982). These indicators of gas hydrates (BSRs) are located in the lower section of the landward slope of the trench. Based on the reported BSR distribution, only the portion of the Nankai Trough seaward of the 1,600 m isobath was included in this study. The southern flank of the central and western trough displays a smooth transition into the abyssal plain of the Shikoku Basin (Figure 1). The eastern limit of the study region is the Zenisu Ridge. The Kyushu-Palau Ridge constitutes the western limit of the Nankai Trough. The eastern area of the trough ends in the vicinity of the Nishishichto Ridge which strikes north to south. This ridge is also known as Izu-Bonin Ridge. The entire area as outlined above is approximately 450 km long with the width varying from 20 to 60 km.

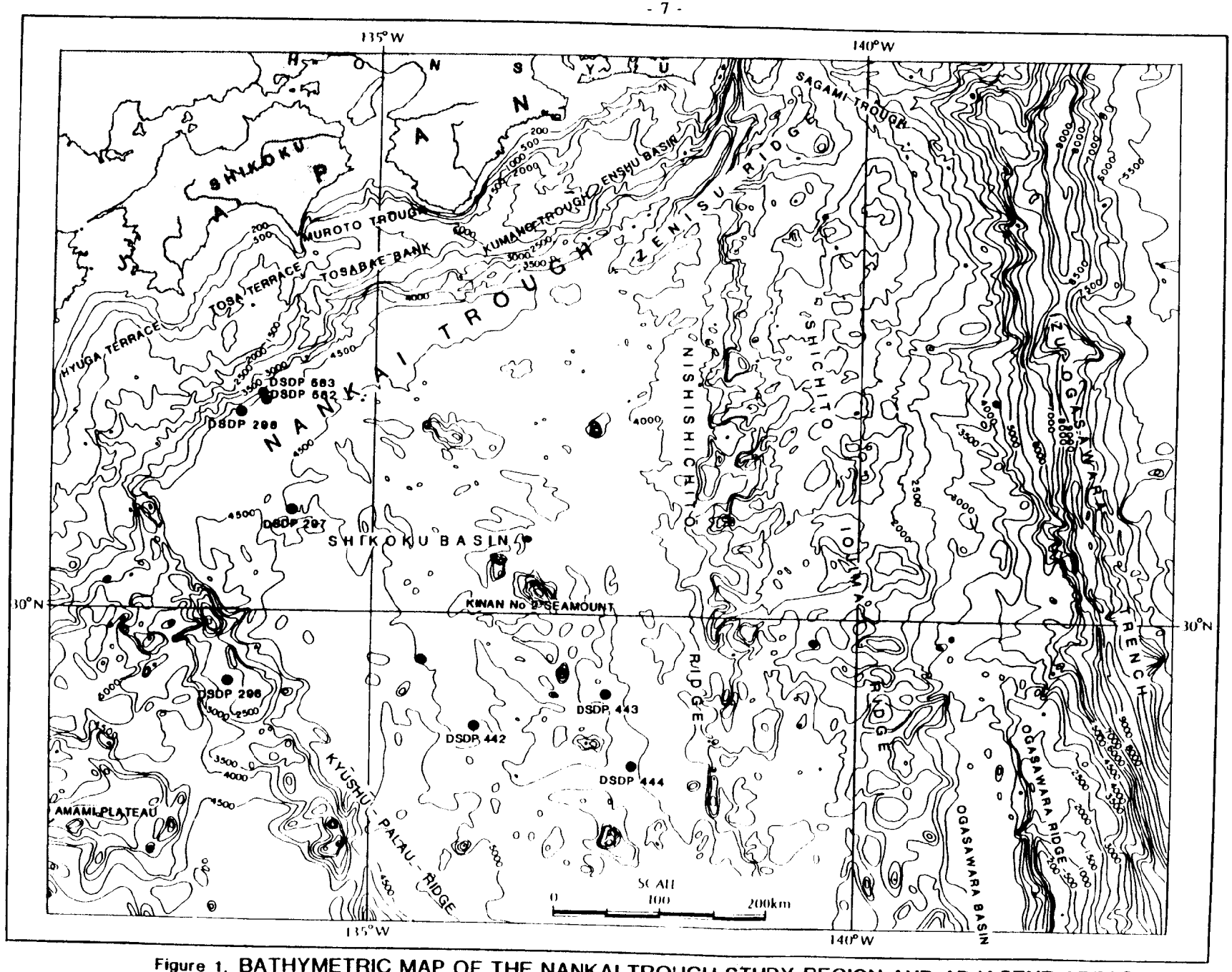

Figure 1. BATHYMETRIC MAP OF THE NANKAI TROUGH STUDY REGION AND ADJACENT AREAS.
After Inoue and Honza, 1982.

Geomorphology

Nankai Trough jointly with the landward slope constitute the continental margin of southwest Japan. This continental margin includes the areas east of Kyushu, south of Shikoku, and the Kii peninsula of the Honshu island (Nankai), as well as east of the Kii peninsula. A narrow continental shelf is found offshore of southwest Japan. Periodic seismic uplifts of coastal promontories, in conjunction with the subsidence of the sea floor, have resulted in deep embayments of the shoreline (Kaneko, 1966).

Two geomorphologically distinct sections of the continental slope are easily discernible in the area adjacent to the Nankai Trough. The upper and lower slope sections are separated by a discontinuous series of flat-surfaced terraces. The terraces occur at a sea depth between 200 and 1,200 m. The upper slope section has a mostly uniform and only a slightly geomorphologically differentiated surface, but the lower slope displays a more diverse relief. The most noticeable feature of the lower landward slope area along the Nankai Trough is the presence of a series of ridges parallel to the trough (Figure 1). The ridges emerge along thrusts rooted in the basal detachment beneath the slope, and thus appear to be structurally controlled. Even a cursory review of the seismic sections presented by Aoki et al. (1982) reveals distinct differences in geomorphological features of western and eastern parts of the lower slope. A typical example of geomorphological features from the western slope is shown in Figures 2 and 3. The seismic line shown in Figure 2 is perpendicular to the Nankai Trough about 70 km southwest of DSDP Site 298. In general, the sea floor dips at a relatively low angle toward the Nankai Trough. With the exception of three pronounced elevated ridges (between points C and D in Figure 2), the seismic line displays much lower surface relief.

Recently elucidated structural controls can explain the present geomorphological features of the trough region. Well developed imbricated sediment wedges and thrust-faulted ridges are easily discernible, particularly at the base of the slope. The ridges were produced by the thrust faults, which in turn were originated by accretionary processes. The ridges appear to be regularly spaced 15 to 2 km, from one another. The ridges rise 100 to 300 m above small intervening depressed areas. Seismic sections reveal that initially a large amount of sediment deformation occurred at the base of the trench slope whereas much less deformation occurred within landward accreted sediment. The nature of the pronounced ridges in the vicinity of Tosa terrace (Figure 2) is not adequately known. It has been suggested (Ludwig et al., 1973) that they represent igneous rock bodies.

The ridges stretching along the Nankai Trough form barriers to sediment transport down the slope. As a result, the depressed areas between the ridges are being progressively filled up. Geomorphologically these areas are represented by flat surfaces (Figure 2). Similarly, with the exception of the accretionary prism, the area of the Nankai Trough is characterized by lack of deformed sediments what is reflected by the almost flat sea floor (Figure 2).

The eastern part of the Nankai Trough displays a different geomorphological pattern (Figures 2 and 3). The eastern section of the Nankai Trough has a steeper

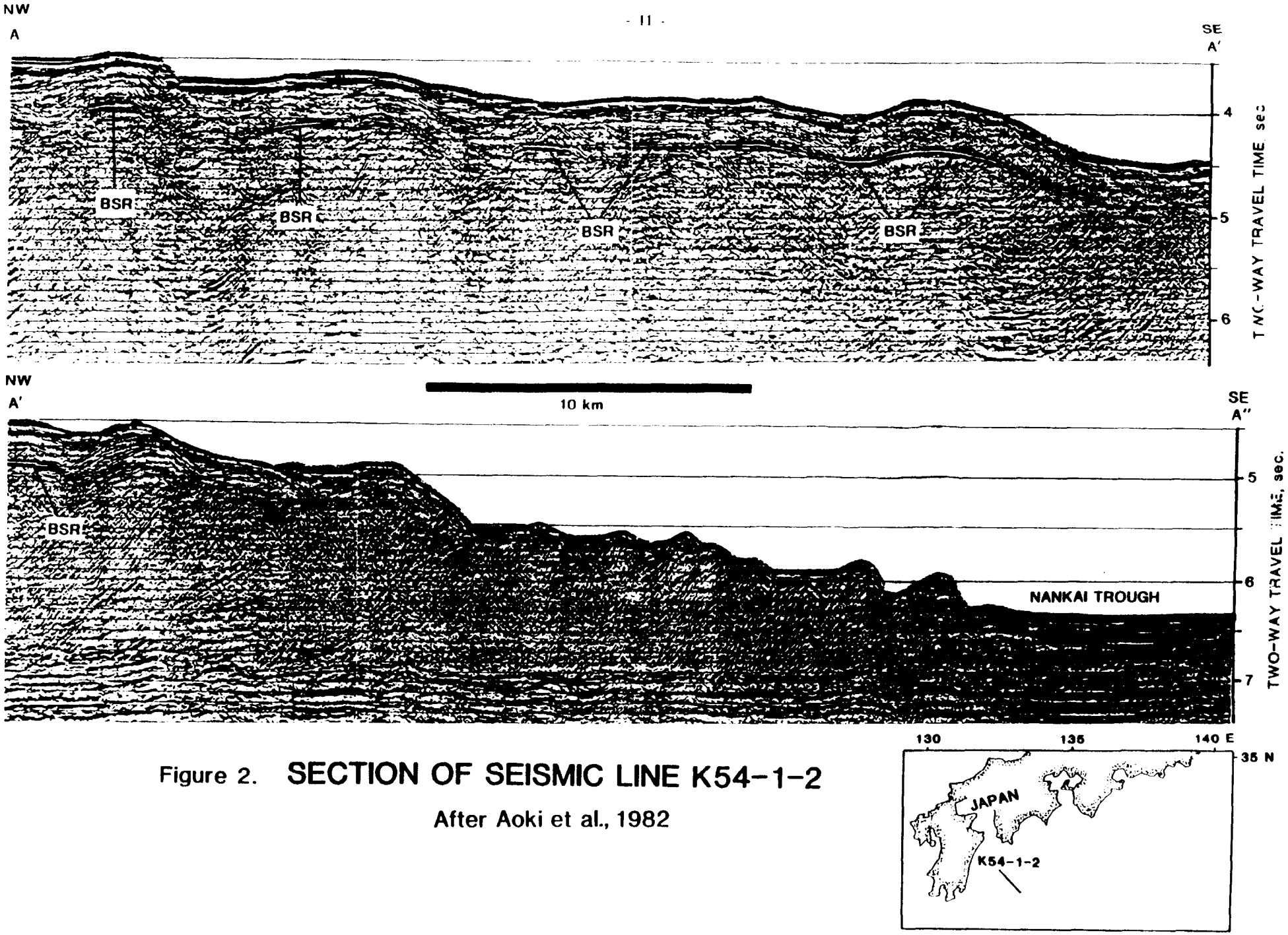

Figure 2. **SECTION OF SEISMIC LINE K54-1-2**

After Aoki et al., 1982

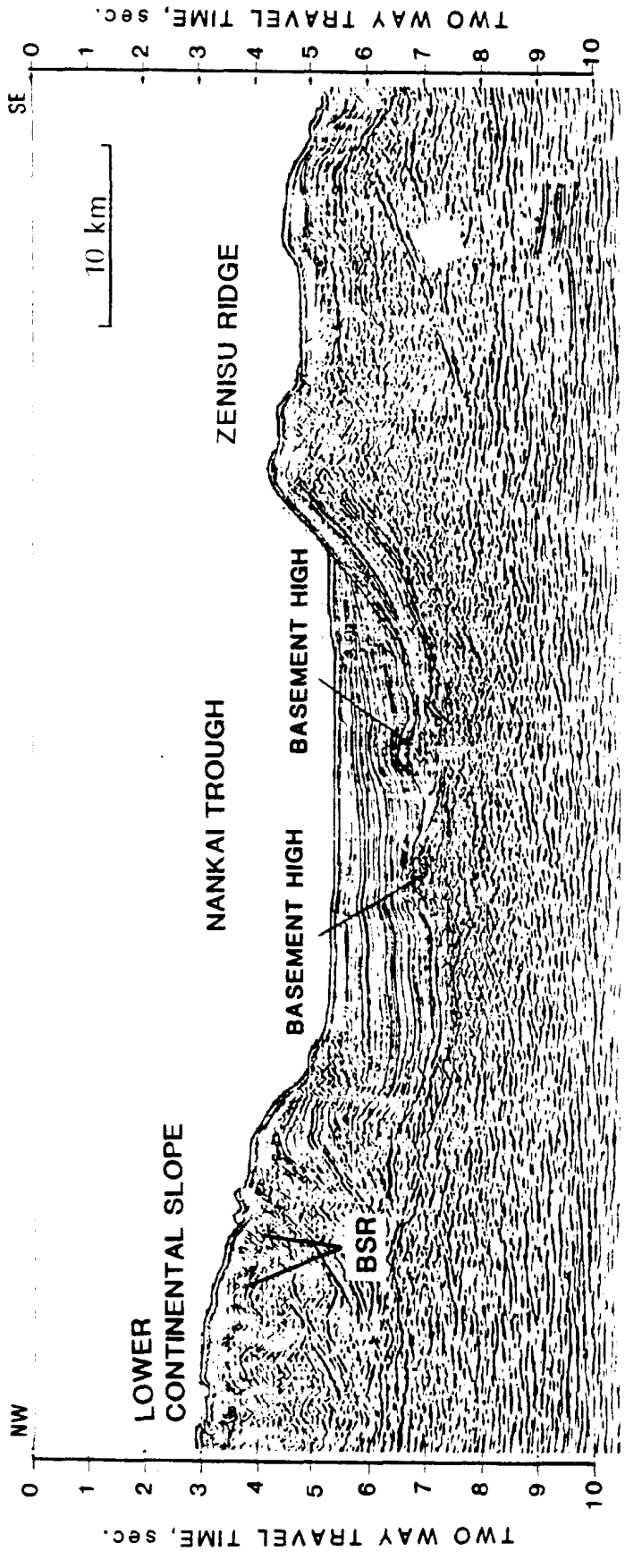

Figure 3. MIGRATED SECTION OF S-4 LINE SHOWING DEFORMATION OF THE LOWER SLOPE AND BASEMENT HIGHS BENEATH THE NANKAI TROUGH

After Aoki et al., 1982

trench slope, thicker trench fill, and greater subduction rate compared with the western section of the area. Some differences in seismology of both areas were indicated by Yamazaki et al. (1980), Hirahara (1980), and others. As a result of the morphological differences, the accretionary complex is thicker in eastern Nankai Trough than in the western part. Aoki et al. (1982) pointed out that faulting of the thick masses of sediments of the eastern accretionary complex indicates much stress. Therefore, the compressional forces have been compensated by folding of the upper, more plastic sediments. Thrusting of the lower strata produced faults spaced at much larger intervals (approximately 10 km) than in western Nankai Trough. Another result of the greater stress needed to deform the accretionary complex is the Zenisu Ridge which accommodates the subduction forces on the seaward side of the eastern Nankai Trough.

Geomorphology of the eastern Nankai Trough is directly related to the tectonic structural features of the area which have been briefly discussed above. Major geomorphological expressions are very pronounced and widely spaced ridges (Figure 3) accompanied by thrust faults. The general dipping trend of the continental margin of eastern Nankai Trough appears to be much steeper compared to its western section. Zenisu Ridge (Figure 1) constitutes a very distinct feature of the eastern Trough. The relative height of this ridge above the surrounding sea floor is approximately 250 m. Although the currently available resolution of seismic sections does not permit determination of the structure of this feature, the explanation summarized in the previous paragraph appears to be quite reasonable.

Structural Setting

Tectonically the Nankai Trough is part of a complex area of active margins marked by a well developed system of trenches. Although its western and eastern limits are delineated by ridges, the Nankai Trough continues to the southwest as Ryuku trench. In an eastern direction it merges at the triple junction with the Japan trench (also known as Shikoku Trench) from the north and the Mariana-Izu trench from the south. The system of trenches mentioned above, south and east of the Japan islands, separates three major tectonic plates in the region, the Pacific plate, the Eurasia plate, and the Philippine plate.

Despite significant advancements during the past 15 years in understanding the subduction mechanisms in actively converging margins, the structural features of those margins still remain relatively obscure. Only recently developed migrating techniques in seismic data processing permit elucidation of some structural problems in the areas of active margins. Some of these migrated records were published by Aoki et al. (1982). Further geological investigations of the area followed during Leg 87A of the Deep Sea Drilling Project, which had as its principal objective the investigation of structural, physical and mechanical properties associated with the subduction zone at the foot of the inner slope of the Nankai Trough. Holes were drilled at Sites 582 and 583 in order to verify previously suggested structural features.

The Nankai Trough is a relatively shallow trench (approximately 4,700 m) due to the subduction of young Miocene crust of the Shikoku Basin. Aoki et al. (1982) cited four major differences between the Nankai Trough and the Japan, Izu-

Mariana, and Ryuku trenches mentioned above. The first distinct feature of the Nankai Trough is Zenisu Ridge extending for about 400 km along the southern flank of the trough. The height of the ridge declines to the west from 1,000 m in its eastern part until it disappears south of the Kii peninsula. The axis of the Zenisu Ridge is only 30 km south of the axis of Nankai Trough. Western Nankai Trough is broad and without an outer ridge. The second difference between Nankai Trough and the other trenches is lack of normal faults in the seaward trench slope. The third difference had been noticed in reference to seismicity and focal mechanisms. The Benioff zone in the Nankai Trough cannot be easily delineated as the distribution of deep focus earthquakes appears not to be concentrated in a narrow zone. Based on the seismological data from the area, it has been suggested that the Benioff zone is gently inclined in the western Nankai Trough while it is much steeper in the eastern trough (Oida and Aoki, 1980). The maximum depths of the Benioff zone in the Nankai Trough are very shallow (approximately 50 to 80 km) compared to the other trenches in the northwestern Pacific. Kanamori (1972) had shown that the earthquakes along the Nankai Trough are of the thrust type, thus confirming that subduction is taking place. The fourth distinct feature of the Nankai Trough compared with the other trenches is relatively high heat flow. The values of the heat flow obtained by Wantabe, Langseth and Anderson (1977) ranged between 2 and 3 HFU.

Despite the apparent differences between the Nankai Trough and others in the region, seismic records disclosed a number of common structural features. One of these features is oceanic basement extending from the trench beneath the landward slope. Among the other characteristic features are folded trench-fill turbidites characteristic of areas with compressive stress associated with subduction.

On the basis of presently available seismic and drilling data, four structurally distinct zones in the accretionary prism of the Nankai Trough have been distinguished (Karig, 1985; Kagami, 1985). These zones are: the protothrust zone, frontal thrust zone, thrust slab 2, and undivided interior sections of the prism (Figure 4).

Protothrust Zone.

In this zone, trench-fill strata appears to thicken landward. A series of steep (60°) landward-dipping seismic discontinuities extend downward through the sedimentary sequences and die out near the contact with the underthrusting Shikoku basinal strata. According to Karig (1985) the protothrust zone begins about 2 km northwest of DSDP Site 582 with a 20 m step or flexure representing the deformation front which extends through the entire trench fill. At the deformation front the uppermost trench turbidites onlap and/or change facies to hemipelagic deposits. At the rear edge of the protothrust zone, at least 40 m of the top of the trench fill are missing or very highly condensed. In contrast to the landward thinning of the uppermost turbidites, the deeper units in the trench wedge display an landward thickening across the protothrust zone. This thickening may be caused either by tectonism responsible for deformation and uplift of the trench fill or as a result of the continuous landward increase in dip of the descending plate (Hsu and Ryan, 1972). The amount of thickening caused by the increase in plate dip depends

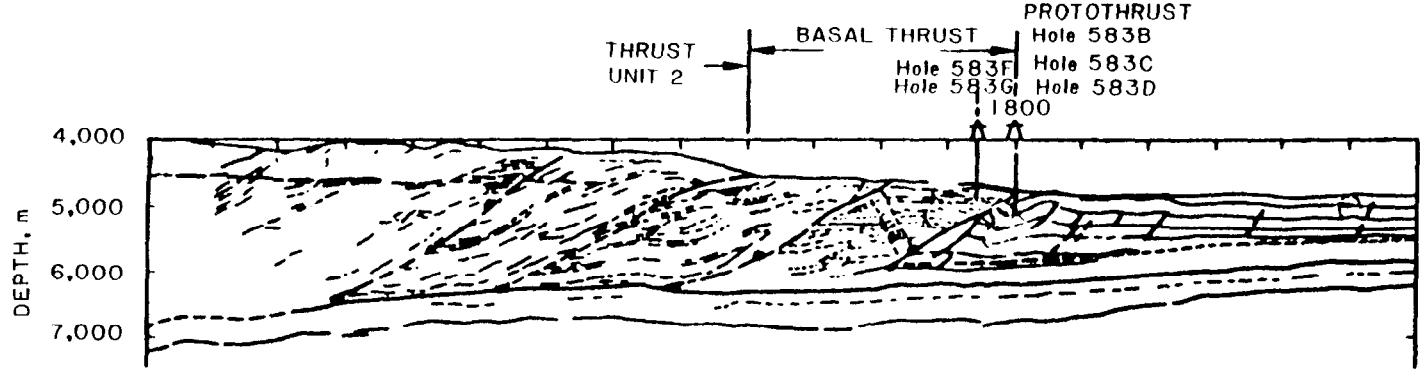

Figure 4. **INTERPRETATIVE DEPTH SECTION ACROSS THE TOE OF THE NANKAI TROUGH ACCRETIONARY PRISM BASED ON SEISMIC PROFILE N 55-3-1**

After Karig, 1986

on rates of deposition and subduction as well as on the differential compaction of the sediment body. Despite the different rates of sediment thickening due to varying rates of deposition and subduction, this general pattern is distinguishable throughout the entire Nankai Trough.

Frontal Thrust Sheet.

The protothrust zone (Figure 4) is abruptly terminated landward by the development of the frontal thrust fault. This feature encompasses the most recent slice of the trench-fill sediments accreted to the southwest Japan arc. This slice has been lifted into a terracelike configuration. The thrust rises upward at an angle of approximately 300 m from the decollement zone which lies 200 m above the Pliocene turbidite sequence (Figure 4). The shallowest segment of the fault surface is not well defined by either seismic or drilling data, but appears to be subhorizontal.

The geometry over the upper 700 to 800 m of the trace of the frontal thrust is clearly discernible on seismic records and drill data. Above the ramp, the hanging-wall strata do not show folding. Over the top of the ramp, however, and southward of the upper ramp corner, the strata in the hanging wall form a south-dipping monocline with dips of 25 to 50°. Folding in this setting contrasts with lack of disturbance along the deeper sections of the thrust, and has been explained by development of a hanging-wall anticline over the upper corner of the thrust ramp. Thus, the geometry of deformation in this area resembles that of the bedding-plane step thrust belts.

Thrust Slab 2.

The frontal thrust slab is backed by another thrust fault, which displays much greater relief and displacement. Bedding plane step thrusts can be observed in thrust slab 2. Strata in the footwall are almost horizontal, whereas those of the hanging wall are almost parallel to the fault surface. Total slip along the fault is about 2.5 km. Again this fault appears to flatten upward into the bedding of the footwall. The uppermost strata of the footwall overlies deeper, steeper-dipping strata in angular unconformity and may represent a section of slope deposits overridden by the thrust for a distance of more than 1 km. Landward of this major thrust, the seismic reflectors within the accretionary prism are more degraded, and only short reflecting segments can be observed. Strata within the hanging-wall slab above the ramp have an average 20° landward dip, attributed to the displacement along the footwall ramp. These reflectors flatten landward of the ramp and terminate at yet another thrust.

Interior Section of the Accretionary Prism.

In the landward direction scattered reflectors which probably represent bedding reach dips of 30°. These reflectors appear on seismic records at subbottom depths less than 0.5 km. A seismically featureless area occurs below 0.5 to 1 km of depth. It is probably a result of continued deformation of the accreted sediments which produced an acoustically white and dispersive environment.

Lithostratigraphy

Knowledge of the lithostratigraphy of the Nankai Trough and adjacent continental slope is still somewhat fragmentary since it is based on seismic records and drilling data from four DSDP sites 297, 298, 582 and 583. Although the understanding of structural features of the active trenches has been steadily improved during the last decade, the more detailed structural picture of the Nankai Trough was derived only in recent years (Aoki et al., 1982). This was possible because of notably improved resolution of seismic sections obtained by migration techniques. As a result, a number of previously unseen structural features, particularly in the outermost accretionary wedge of the trough, have been identified. One of the major goals of the drilling activities in the area of the Nankai Trough within DSDP Legs 31 and 87 was to obtain direct data to verify previous seismic interpretations as well as to develop a consistent model of sedimentological and structural development of the Nankai Trough. During Legs 31 and 87, holes were drilled at two sites located within undeformed (Site 297 and 582) and two in deformed (Site 298 and Site 583) belts of the trough sediments (Figure 1; Table 1).

DSDP Site 297

The site is located in the northwestern corner of the Shikoku Basin on the outer arch of the Nankai Trough (Figure 1). Two holes were drilled at this site. With water depth of 4,458 m, the maximum penetration of 679.5 m into the sediments was reached in hole 297. Sediments ranging in age from Pleistocene to middle Miocene were identified in this drill hole (Figure 5). Five lithologic units were discerned by Ingle et al. (1975):

Unit 1 (0 to 47 m) consists mainly of diatom/ash clay. Diatom content ranges from 5% to 44% while the calcareous nannofossils make up less than 1%. Silt-sized glass and volcanic feldspar are another major lithological element making up 15% to 93% of the sediment. Volcanic ash occurs as small pods and up to 0.5 m-thick beds. The prevailing color of Unit 1 is olive-gray.

Unit 2 (47 to 85 m). In contrast to Unit 1, this interval is represented by clay-rich nannofossil ooze with 15% to 72% nannofossils. Downward in Unit 2, the sediments become more clayey. Volcanic ash was found in all rock samples in

TABLE 1.

SUMMARY DATA ON DSDP DRILLING SITES IN NANKAI TROUGH

DSDP Site	Location	Ocean depth m	Thickness of penetrated sediment m	Age of the oldest sediment
297	30°52.36'N 134°09.89'E	4458	679.5	Early mid Miocene
297A			200.5	"
298	31°42.93'N 113°36.22'E	4628	611	Early Pleistocene
298A			98	"
582	31°46.51'N 133°54.83'E	4892	29.1	Quaternary
582A	31°46.51'N 133°54.83'E	4879	48.5	Quaternary
582B	31°46.51'N 133°54.83'E	4892	749.4	Pliocene
583	31°50.00'N 133°51.40'E	4634	152	Quaternary
583A	31°50.18'N 133°51.26'E	4618	54	Quaternary
583B	31°49.76'N 133°51.26'E	4677	30	Quaternary
583C	31°49.80'N 133°51.26'E	4677	49	Quaternary
583D	31°49.76'N 133°51.54'E	4676	326.6	Quaternary
583E	31°50.10'N 133°51.30'E	4629	198.7	Quaternary
583F	31°51.10'N 133°51.30'E	4629	439.7	Quaternary
583G	31°50.07'N 133°51.40'E	4627	450.7	Quaternary

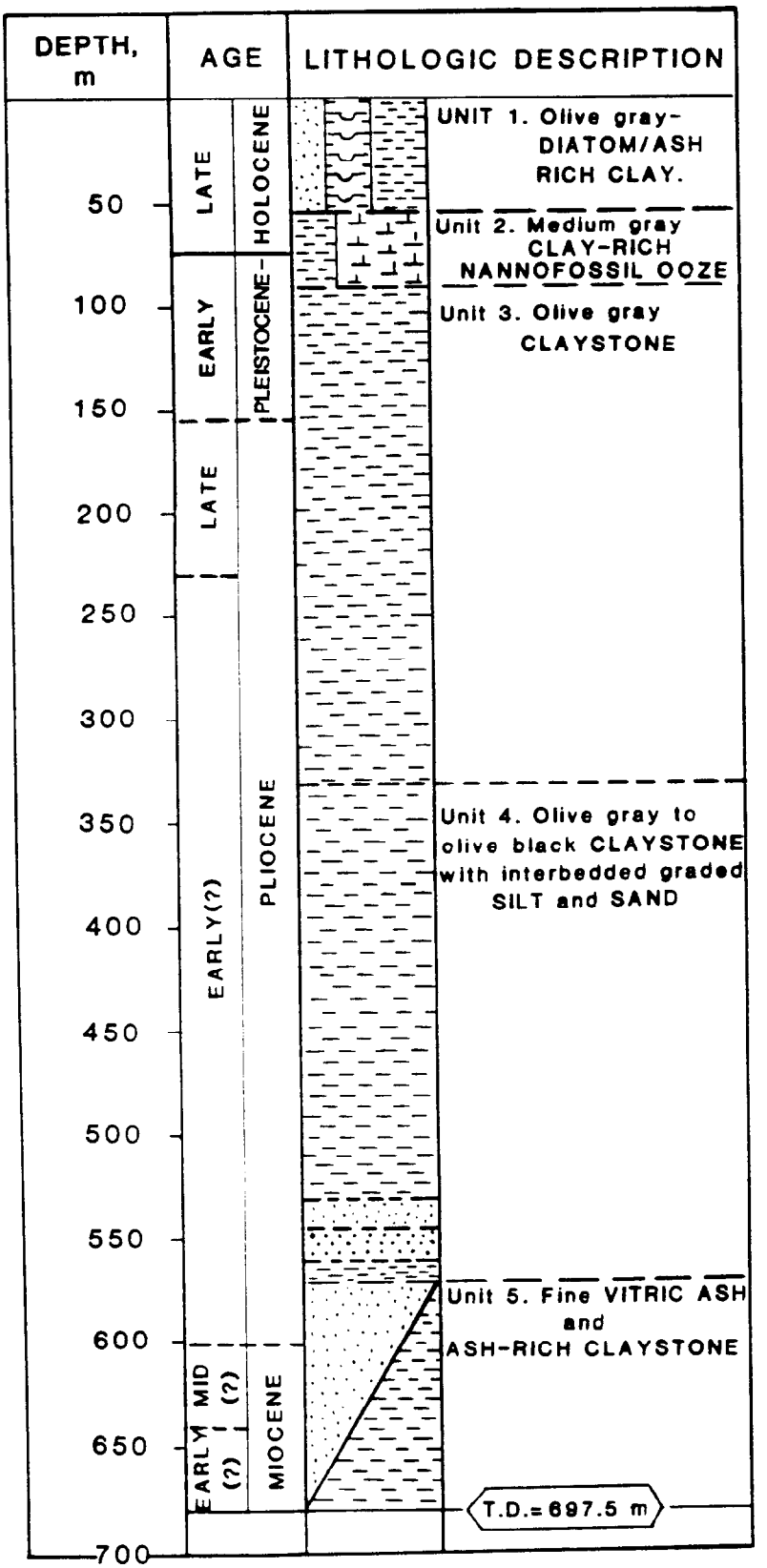

Figure 5. LITHOSTRATIGRAPHY OF DSDP SITE 297

After Ingle et al., 1975

quantities of 10% to 20%. Also a few thin lenses of vitric ash have been identified. Medium gray color dominates throughout the entire interval.

Unit 3 (85 to 325 m). The sediments of Unit 3 are mainly composed of an olive-gray semilithified clay and silty clay with a few fossils present. Although some thin beds were found in the interval, generally the ash content is very low. The entire unit is significantly more consolidated than the two overlying units.

Unit 4 (375 to 578 m). The most distinct feature of this unit is the presence of thin (less than 0.3 m) graded beds of silt and fine sand, presumably turbidites within mostly olive-gray to olive-black claystone. Ash and fossils are either absent or their presence was found to be in trace amounts. The presence of some pyrite and glauconite have been documented. Commonly occurring fine plant debris indicate onshore provenance.

Unit 5 (578 to 679.5 m) is composed of fine vitric ash to ash-rich claystone. Graded beds at the top of the unit containing pyrite and plate debris had been interpreted as distant turbidites. The laminae of vitric ash indicated intense slump structures in several zones.

DSDP Site 298

The site is located on the lower, inner slope of the Nankai Trough of Shikoku Island (Figure 1). The corrected water depth at the site is 4,628 m. Out of two holes drilled at this site, the maximum depth of penetration (611 m) was reached in borehole 298 while the second hole (298A) penetrated only 98 m of sediments. In hole 298, the stratigraphic sequence consists of 183 m of Holocene to late Pleistocene turbidite clayey and silty sand, and silty clay underlain by 427 m of late to early Pleistocene clay, silt and clayey-silty sand (Figure 6). In hole 298, two lithologic units were distinguished:

Unit 1 (0 to 188 m) is composed mainly of clayey silt and clayey-silty sand with minor amounts of small cobbles of silty claystone, calcareous sandstone and limestone. Granules and sand-size lithic fragments were found in sand beds. Cobbles usually occur in the form of irregular-sized clasts. Some of them show features of weathering. Sand in Unit 1 is medium to fine-grained, and occurs in beds up to 1 m thick. The foraminifera in Unit 1 were found reworked from the neritic zone, most likely by turbidity currents.

Unit 2 (188 to 611 m) differs from the overlying unit by lack of cobbles. The principal lithologies encountered in this interval were fissile clayey silt and silty clay. Also some volcanic ash and nannofossils with traces of radiolarians, sponge spicules and diatoms were found. Sand and silt layers occur in 70% of the cores recovered from the Unit 2 interval. The sands, with up to medium grain size, occur in beds up to 16 cm thick. The type of grading and poor sorting within the beds indicate that silts and sands of Unit 2 were deposited by turbidity currents. Volcanic ash layers up to 9 cm thick have been also identified in this unit.

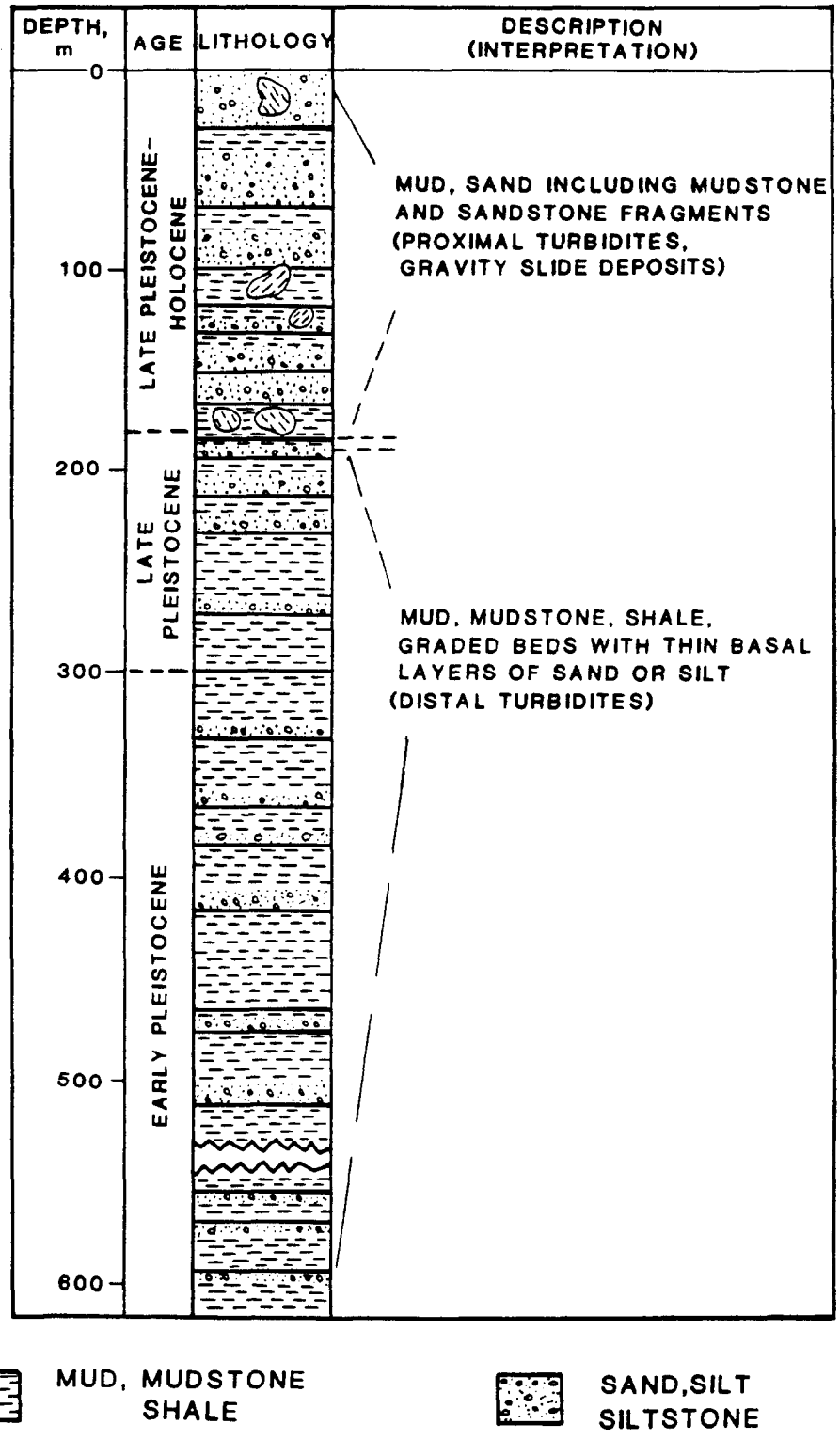

Figure 6. LITHOSTRATIGRAPHY OF DSDP SITE 298

After Ingle et al., 1975

DSDP Site 582

Site 582 is located within the undeformed sediment portion of the Nankai Trough in close proximity to the major subduction thrust (Figure 1). The water depth at this location is approximately 4,880 m. The maximum subbottom penetration depth of 749.4 m was achieved in hole 582B, where the oldest sediments proved to be of Pliocene age. The lithologic profile at Site 582 reflects the deposition of hemipelagic sediments, eolian sedimentation from volcanic episodes on the Japanese island arc as well as sediment gravity flows. Generally two lithologic units had been discerned in hole 582. The distinction is based mainly on the sand content. Sand layers are more frequent in the upper 530 m (Unit 1) of the column while the lower sections (Unit 2) are virtually devoid of sand. According to the sand percentage, nine subunits (four sandy and five muddy) are distinguishable with Unit 1. Volcanogenic plagioclase and glass were found throughout the entire unit with a slight trend to increase at the top of the two main lithologic units.

Unit 1 (0 to 566 m) consists of dark olive-gray hemipelagic mud intercalated with sandy and silty layers. Such lithological composition was found to be typical for most circum-Pacific trench axes and landward slopes (Aubouin et al., 1982). Hemipelagic mud of Unit 1 also contains silt-size grains and varying amounts of microfossils. In general, siliceous microfossils prevail over calcareous. Diatoms were found mostly within the 0- to 425-m subbottom depth interval. Beneath this interval their occurrence is insignificant. While sponge spicules show up in the form of white patchy concentrations, radiolarians are common in the muds in the immediate intervals beneath coarser-grained strata. Volcanic ash was found to be disseminated throughout the entire unit, occasionally reaching 40% to 50% of the sediment bulk. Sand and silt are frequent lithologic components of Unit 1. Numerous sandy intervals were encountered at a subbottom depth of 25 to 125 m. In some of these intervals grading was identified. Below the subbottom depth of 125 m to 325 m, the sediments become silty. The interval from 325 to 470 m consists of pumice-bearing graded sands. A variety of heavy minerals were identified within sand and silt formations of Unit 1. Among the most frequent are hornblende, biotite, apatite, pyroxene and zircon. Estimates of the sand fraction within coarse-grained beds suggest a general downhole decrease of sand content from 0 to 300 m. Among the biogenic components of the sandy intervals, foraminiferas are the most common. Calcareous benthic foraminifera found in this unit are characteristic of much shallower sea depth than present.

Unit 2 (566 to 749.4 m). The nature of the abrupt lithological change at the top of this unit is not known, due to poor core recovery from the interval. The top boundary delineates the end of mostly hemipelagic sedimentation. While Unit 2 consists of dark gray hemipelagic mudstone, it lacks the coarse-grained constituents of the overlaying Unit 1. Among other features which differ from Unit 2 to Unit 1, Karig et al. (1986) listed slightly green tint and color alterations, lack of graded-bed chondrite sequences, the presence of numerous pumice clasts in a mudstone matrix and sparse occurrence of lighter colored, nannofossil-rich intervals.

DSDP Site 583

This site was located on the deepest terrace of the inner trench slope. The sediments of the accretionary wedge of the Nankai Trough were penetrated to different depths in eight holes spudded in the vicinity of Site 582 (Table 1). In four holes (583, 583A, 583B, and 583C), the sediments were cored using a hydraulic piston corer, while in the remaining four holes (583D, 583E, 583F, and 583G) rotary coring tools were utilized. Even though the holes were closely spaced, the lithostratigraphic correlation was not possible due to the percentage of recovered cores, nature of the sediments and structural complexity of the area. The recovered cores did, however, provide a general view of lithostratigraphy of the lowermost inner trench slope.

Hole 583 (0 to 153 m). The entire sequence is of Quaternary age. The lithologic profile consists of hemipelagic mud sequence interbedded with graded sands and silts and occasional ash layers. Plant matter was found to be associated with coarser sands. The interval from 0 to 16 m consists mostly of dark gray mud inter-bedded with 40 to 50 cm thick graded silt with sharply defined bases. Calcareous fossils were found only in the coarser sediments. Woody matter was found in visibly graded 110 cm thick dark micaceous sand layer at 16 m. At the subbottom depth of 16 to 32 m, clay sediment fractions gradually increase. Predominantly clay sequences were recovered in cores from the interval 32 to 53 m. Although this interval seems to be a shallow muddy sequence, it is also interbedded by thin, very dark gray, graded silts. Further down the hole to the depth of 61 m, the mud becomes more silty. Sediments at the interval 62 to 73 m contain less clay fraction and consist mainly of muddy pumice-rich sand with pumice granules, mud clasts, and woody fragments. Beneath 73 m, the core recovery was poor and only a fragmentary data on the lithology were obtained. Recovered cores contained mostly hemipelagic muds, occasionally silty with dark gray layers of silts and sands 5 to 45 cm thick.

Hole 583A (0 to 54 m). As in hole 583, the hemipelagic mud sequence contains commonly occurring silty layers. The latter are usually graded and have sharp erosional bases. Pyrite is frequently present in the lower parts of these layers. Plant fragments were also noted while some muds were found to be mottled with black, most likely organic-rich material. Pale yellow authigenic calcium carbonate concretions or crystalline aggregates were also identified in these sediments.

Hole 583D (46 to 327 m). Knowledge of the lithological sequence at this location is mostly based on 25%-recovery rotary cores. The entire section consists predominantly of dark gray hemipelagic mud with some graded silts and rarely occurring coarse sands. Plant matter commonly occurs in the sand layers. No ash or carbonate layers were identified in this profile.

Hole 583F (150.4 to 439.7 m). The lithology consists mostly of dark gray hemipelagic muds of Quaternary age, interbedded with graded silts and sands and

occasionally with coarse sands with pumice and plant fragments. Chondrites were found in sediments below 257 m, nannofossils are abundant in many clay intervals.

Sedimentation

Drilling activities during DSDP Legs 31 and 87 provided valuable but somewhat limited insight into the sediments of the Nankai Trough and the adjacent lowermost continental slope. As the known bottom simulating reflectors (BSRs) in the area occur in the mid-lower continental slope, the lithostratigraphy documented from the "nearby" DSDP sites can only be applied to the subject of gas hydrates in a broad sense.

Two principal types of sedimentation have been discerned on the basis of lithological profiles, both in deformed and undeformed sediments of the Nankai Trough (Taira and Niitsuma, 1986). The turbidite sequences, represented by interbedded sandstone and shale with turbidite sedimentary structures, appear to form the upper 500 m of the sedimentary profile. The lower sedimentary unit consists predominantly of hemipelagic muds.

Turbidite Sequence

A turbidite bed is typically composed of three subunits: lower graded sands, upper massive silts, and uppermost chondrite-burrowed silts. The sediments of the upper 300 m of DSDP Site 582 are poorly known due to low core recovery. The sediments beneath 300 m show lithological sequences as well as structures typical for turbidite sedimentation. Four lithological divisions can usually be distinguished in the turbidite sequences (Taira and Niitsuma, 1986; Figure 7). The first division T_1 consists of massive to graded sands. The sands appear to be poorly sorted while mud content does not exceed 10%. The grain size in this formation ranges from coarse to fine. Other components found in the T_1 division are pumice and plant fragments (including stems of land plants). The second subunit (T_2; Figure 7) of the turbidite sequence is characterized mainly by structureless, and occasionally parallel, finer laminated sands and silts. Increased amounts of microfossils were noted toward the top of this subunit. Such a pattern is particularly noticeable in calcareous nannoplankton. Another important marker for depositional environment is diatoms. All these observations suggest the shallow nearshore sedimentary environment for the sands encountered at Site 582. The third subunit of the turbidite sequences (T_3; Figure 7) is represented by silts with an abundance of chondrite burrows. The uppermost subdivision of the sequence (H; Figure 7) consists of greenish blue mud which is commonly burrowed. The apparent absence of calcareous nannofossils and subsequent low calcium carbonate content was interpreted by Taira and Niitsuma (1986) as due to $CaCO_3$ dissolution. The same authors suggested that hemipelagic muds of subunit H were deposited relatively slowly below the calcite compensation depth (CCD).

The turbidite sequences of DSDP Site 583 are different from those at Site 582 (Figure 8). Typically three subunits sequences are discernible at Site 583 (Taira and Niitsuma, 1986). Subunit T_2 consists of dark olive gray silt and very fine-grained sand with parallel lamination. The overlaying subunit T_3 is represented by a

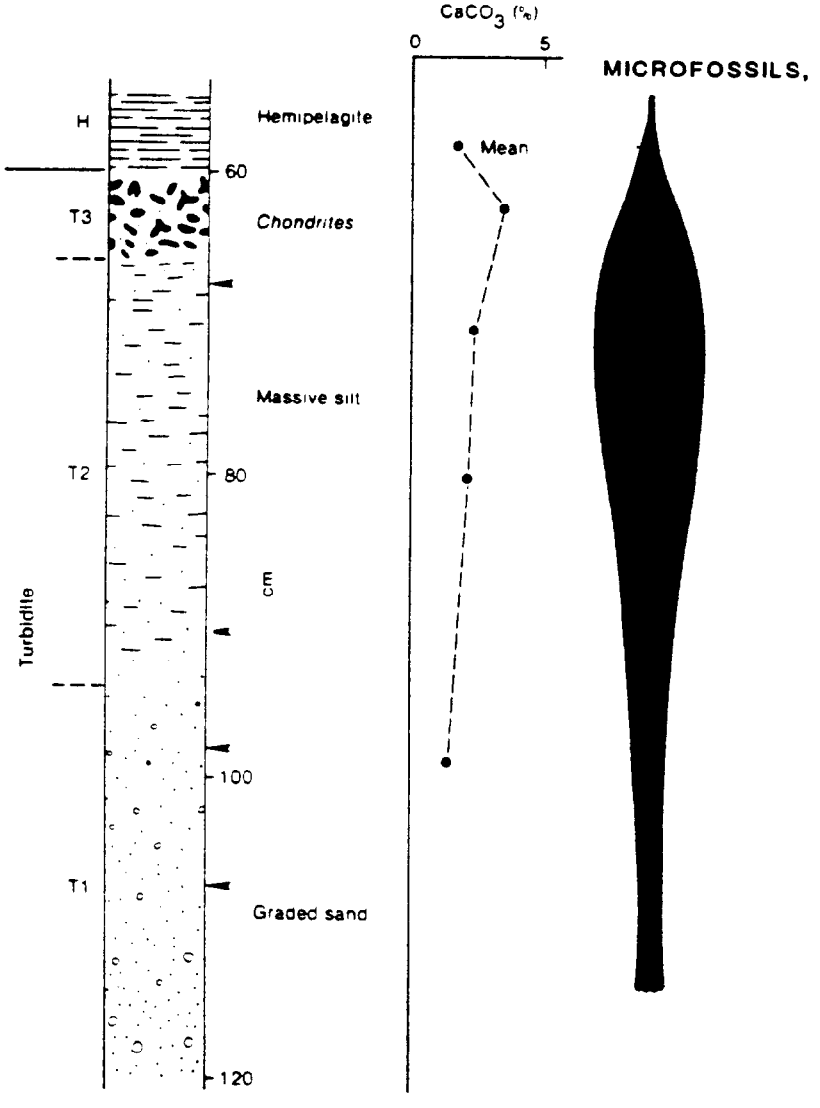

Figure 7. TURBIDITE SEQUENCE FROM DSDP SITE 582B
After Taira and Niitsuma, 1986

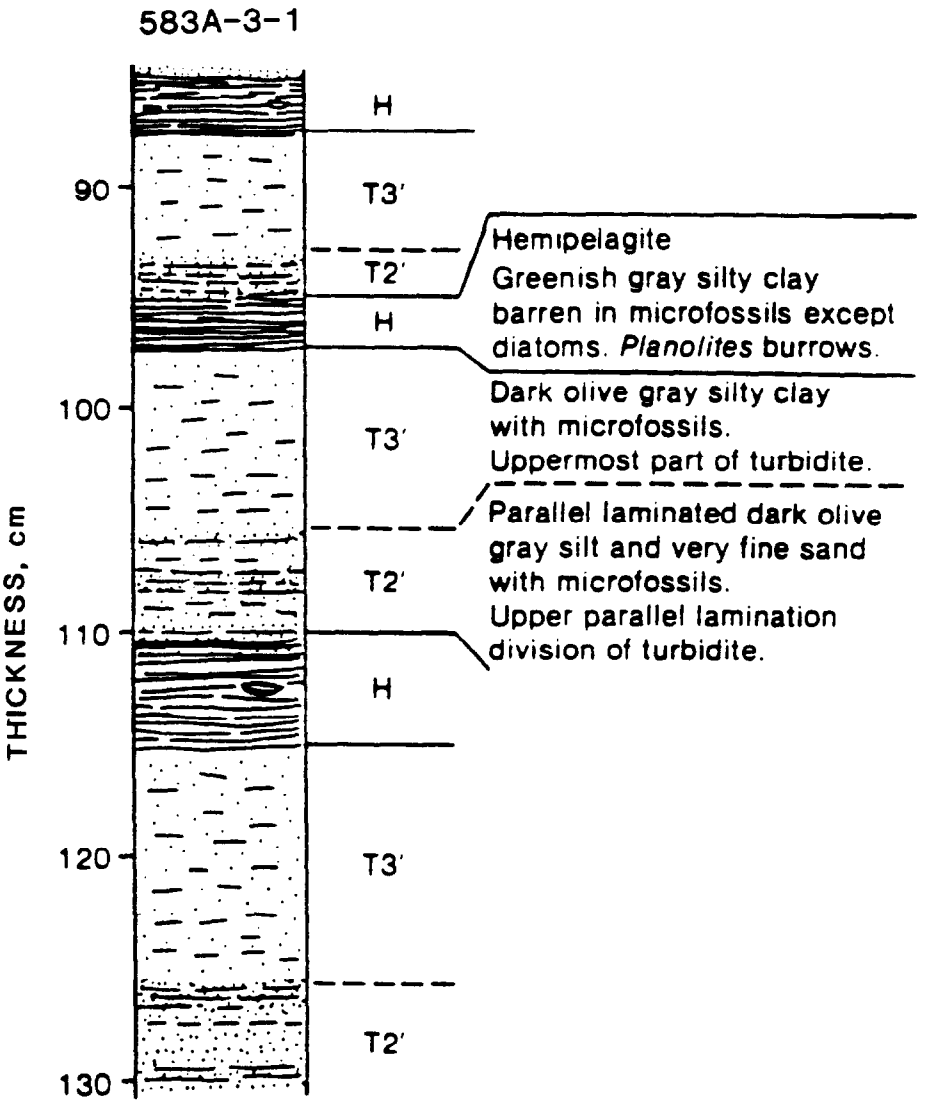

Figure 8. **TURBIDITE SEQUENCES FROM DSDP SITE 583A**
After Taira and Niitsuma, 1986

massive bedding of silty clay with microfossils. The uppermost subunit H appears to be similar to its counterpart at Site 582.

Some important sedimentological aspects of the turbidite deposition in the Nankai Trough were elucidated as a result of detailed analyses of the recovered cores. These analyses involved grain size analysis, bed thickness distribution and magnetic susceptibility. Grain size analysis revealed the following major features of the turbidite beds:

- The sediments are poorly sorted, the grain-size distribution lacks a visible modal peak.
- Grading trend is noticeable in the form of gradual decrease of coarse-grain tail.
- Two distinct grain-size distribution patterns were found in the T_1 and T_2 subunits of the turbidite sequences.
- In contrast to subunit T_2, well developed coarse fractions occur over a wide range of frequencies in T_1.
- The boundary between the two sequences appears to be sharp. Although two patterns probably represent two different depositional regimes, their nature is not quite clear.

Another observation made in turbidite beds of the Nankai Trough is the lack of well developed parallel and ripple lamination. This feature resulted perhaps in sediments which were too fine to form flat beds or current ripples. Available data on grain size of sediments offshore of southwestern Japan show good general correlation between sediment sorting and distance from the islands. The sorting processes were undoubtedly reinforced by the structural features of the continental slope. The exception from this pattern has been found at the Saruga Trough area (Figure 1) where a large volume of nearshore sands has been identified to a depth exceeding 3,000 m. The analysis of lateral changes of grain size in the Nankai Trough, particularly with regard to sorting, supports the idea of sediment transportation from a northeast direction toward the southwest part of the trough.

The bed-thickness distribution of turbidite sequences was examined in cores recovered at Sites 582 and 583 (Taira and Niitsuma, 1986). The thickest turbidite in the two drillholes measured 105 cm with a mean value of 30.2 cm. The mean thickness of the hemipelagic intervals is 6.5 cm where the maximum thickness is 20 cm. The comparison of the bed-thickness distribution at Sites 582 and 583 with other known turbidite sequences led Taira and Niitsuma (1986) to the conclusion that turbidites at Site 582 represent distal channel-levee-overbank association, whereas the sediments in the upper 50 m sequence of Site 583 probably represent an overbank depositional environment. These findings do not appear to contradict the hypothesis about sediments channeled from a northeastern direction.

The analyses of magnetization directions in core specimens from the Nankai Trough were used to decipher depositional paleocurrents (Taira and Scholle, 1979). As the sandy and muddy sequences revealed contrasting magnetic susceptibility directions, the paleocurrent direction was predominantly from northeast to southwest, or parallel to the axis of the Nankai Trough.

Petrographic examination of the turbidite sediments at Sites 582 and 583 supports the suggestion by some authors (Sato, 1962; Ohtsuka, 1980; Taira and

Niitsuma, 1986) of a northeast to southwest sediment transportation pattern. In this investigation area some arguments seem to be particularly noteworthy:

1. Sands encountered at Sites 582 and 583 contain land-derived plants as well as fresh water diatoms. On the other hand, these sediments are devoid of typical marine organism remnants such as skeletal debris of molluscan shells and echinoderm fragments commonly seen in marine sands offshore of the Japanese islands. These observations suggest river mouth provenance of the sediments rather than from shelf areas.

2. Presence of substantial amounts of volcanic components include volcanic rock fragments, pumice, volcanic glass, plagioclase, pyroxene, and olivine. Some of the basic and intermediate volcanic rock fragments proved to be of particular importance in establishing their source location. Red volcanic fragment provenance is limited to two areas in the outer zone of southwestern Japan, Kyushu and central Japan.

3. Micas, hornblende and some other metamorphic minerals perhaps originated from a granitic terrane.

Investigations and comparisons of detrital components of the sands at Sites 582, 583 and surrounding areas enabled Taira and Niitsuma (1986) to distinguish four compositional types of sand provinces in the outer zone of southwestern Japan. Sands from Kyushu Island are characterized by a high amount of acidic volcanic component which is virtually absent in sands originated in Shikoku Island. Sands from Tokai proved to be slightly more feldspathic than those from Shikoku. Finally, sands from the Nankai Trough, Saruga Trough and the Fuji River area were found to be almost identical petrologically.

Underlying turbidite sequences at Site 582 are mainly greenish blue hemipelagic mudstone of Unit 2. Despite lower content of microfossils in the latter formation, locally present calcareous fossils can be interpreted as the indicator of the sediment deposition above CCD depth.

Sedimentary Facies

Turbidite sedimentation as the predominant feature of the Nankai Trough area. The Nankai Trough study region includes an area of approximately 100,000 km^2 of turbidites with an average thickness of 500 m. The transportation of sediments involved distances perhaps as long as 700 km. It has been suggested (Niitsuma and Akiba, 1986) that the enormous turbidite sedimentation was triggered by the Tzu-Honshu collision which began 2 m.y. ago. These events formed a steep drainage system along strike-slip faults which, jointly with supplied clastic sediment, created a major fan-delta system at the river mouth. The slope was occasionally disturbed by earthquake activities. The rapid sediment supply to the trough caused an accretionary prism to form as the sediment could not be completely subducted.

More detailed examination of bathymetric maps and other data obtained in the area, enabled Taira and Niitsuma (1986) to come up with a facies model in the Nankai Trough (Figure 9). The model includes two major mechanisms. One is that trench turbidites are funneled through a longitudinal channel, forming a lenticular

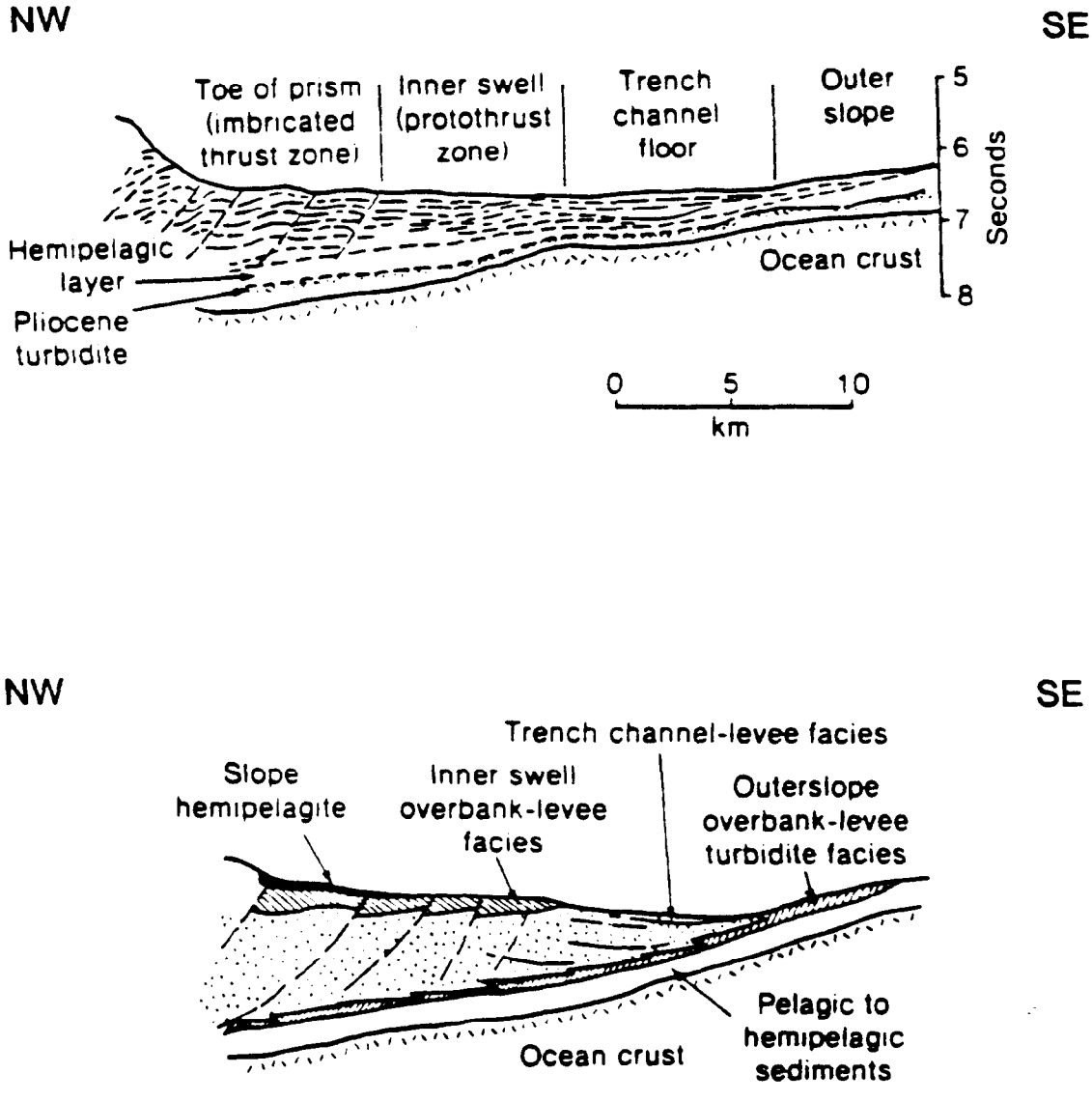

Figure 9. **STRUCTURAL AND SEDIMENTOLOGICAL INTERPRETATION OF REPRESENTATIVE SEISMIC LINE**

After Taira and Niitsuma, 1986

sand body. The second assumed mechanism is that, as the trench-floor elevation gradually increases toward the toe of the accretionary prism, there is a wide zone of 'overbank' deposition where diluted turbidite currents are accommodated. Such a facies pattern implies a fining upward trench-fill depositional cycle. Subsequently the central trough channel facies becomes levee facies and then finer-grained, thin bedded overbank turbidite and slope hemipelagic facies can be observed.

Hydrocarbon Potential

The presence of light hydrocarbons is necessary for gas hydrate formation. Therefore every assessment of gas hydrates must include an analysis of hydrocarbon potential. Presently available petrological and geochemical data from the Nankai Trough are limited to the southwestern and south central part of this area where DSDP drilling Sites 297, 298, 582, and 583 were located. For future reference it is important to remember that while Sites 297 and 583 represent an area of the Nankai Trough floor with undeformed sediments, the remaining Sites 298 and 583 were drilled in the stratigraphically equivalent but deformed sediments of the thrust sheets of the accretionary wedge.

Several analytical techniques for evaluating hydrocarbon source rock potential of rock samples at DSDP sites generated important parameters, including organic and carbonate carbon, kerogen composition, hydrogen and oxygen indices, genetic potential, vitrinite reflectance, and thermal maturity.

Organic Carbon

Organic carbon content is a principal measure of the hydrocarbon generation potential of sediments.

Although some laboratories use 1% total organic carbon as a lower limit for detrital hydrocarbon source rock, the value of 0.5% is commonly accepted (Hunt, 1979; Tissot and Welte, 1978). The total organic carbon content (TOC) in samples collected at DSDP sites in the Nankai Trough are shown in Table 2 and Figures 10 and 11. Organic carbon values of the sediments at Site 582 range from 0.55% to 0.73% in the upper 500 m. Below this depth TOC values were found to be less than 0.5%. This change can probably be correlated with the boundary between trench-fill sediments and hemipelagic deposits related to the Shikoku Basin (Mukhopadhyay et al., 1986). In general, however, the changes in TOC content do not show correlation with sediment lithology. At Site 583, organic carbon was analyzed in sediment samples from drill holes 583, 583B, 583D and 583F (Table 2). With the exception of samples from the depth interval around 100 m where TOC content was 0.38%, all other samples revealed organic carbon values higher than 0.5% (Figure 10). Despite the minor local differences in TOC values, the analyzed sediments display a fairly uniform set of values. Sekiguchi and Hirai (1986) stated that organic matter in sediments at Sites 582 and 583 was deposited in Shikoku Basin in environments similar to those of the present. Total organic carbon values in the analyzed samples appear to be significantly elevated over usual 0.2% values found in the Shikoku Basin (Rullkotter et al., 1980; Waples and Sloan, 1980). The lack of correlation between TOC content and lithology suggests that organic matter

TABLE 2.

CARBON CONTENT OF SEDIMENTS FROM DSDP SITES 582 AND 583.
After Sekiguchi and Hirai, 1986

DSDP Site	Subbottom Depth m	Organic Carbon wt %	Carbonate Carbon wt %
SITE 582	0.00-5.22	0.57	0.03
	29.10-33.42	0.38	0.17
	58.20-61.44	0.68	0.25
	87.30-87.96	0.57	0.19
	116.10-118.63	0.65	0.22
	135.50-142.35	0.67	0.30
	183.60-187.24	0.58	0.19
	212.50-212.97	0.67	0.19
	231.90-232.82	0.59	0.19
	251.10-253.23	0.42	0.02
	279.90-280.53	0.51	0.22
	318.30-319.48	0.65	0.34
	337.50-338.91	0.59	0.23
	365.90-366.61	0.60	0.33
	394.30-394.74	0.49	0.22
	413.20-416.47	0.55	0.29
	432.00-434.50	0.56	0.25
	460.50-461.22	0.58	0.12
	498.60-499.76	0.57	0.14
	537.00-538.79	0.47	0.20
	566.00-568.15	0.35	0.02
	604.50-606.61	0.40	0.10
	623.70-624.18	0.35	0.20
	642.90-643.75	0.46	0.50
	671.80-675.22	0.46	0.09
	691.20-692.67	0.39	0.06
	710.60-712.61	0.36	0.29
SITE 583	5.00-8.25	0.68	0.14
	20.00-22.16	0.61	0.10
	40.00-40.46	0.67	0.13
	66.00-67.78	0.74	1.10
	95.00-97.16	0.55	0.20
	123.70-126.32	0.65	0.21
	152.60-153.98	0.66	0.26
	181.70-182.13	0.59	0.27
	220.20-221.46	0.65	0.02
	249.30-251.06	0.55	0.21
	268.70-274.13	0.53	0.19
	316.90-318.63	0.64	0.23

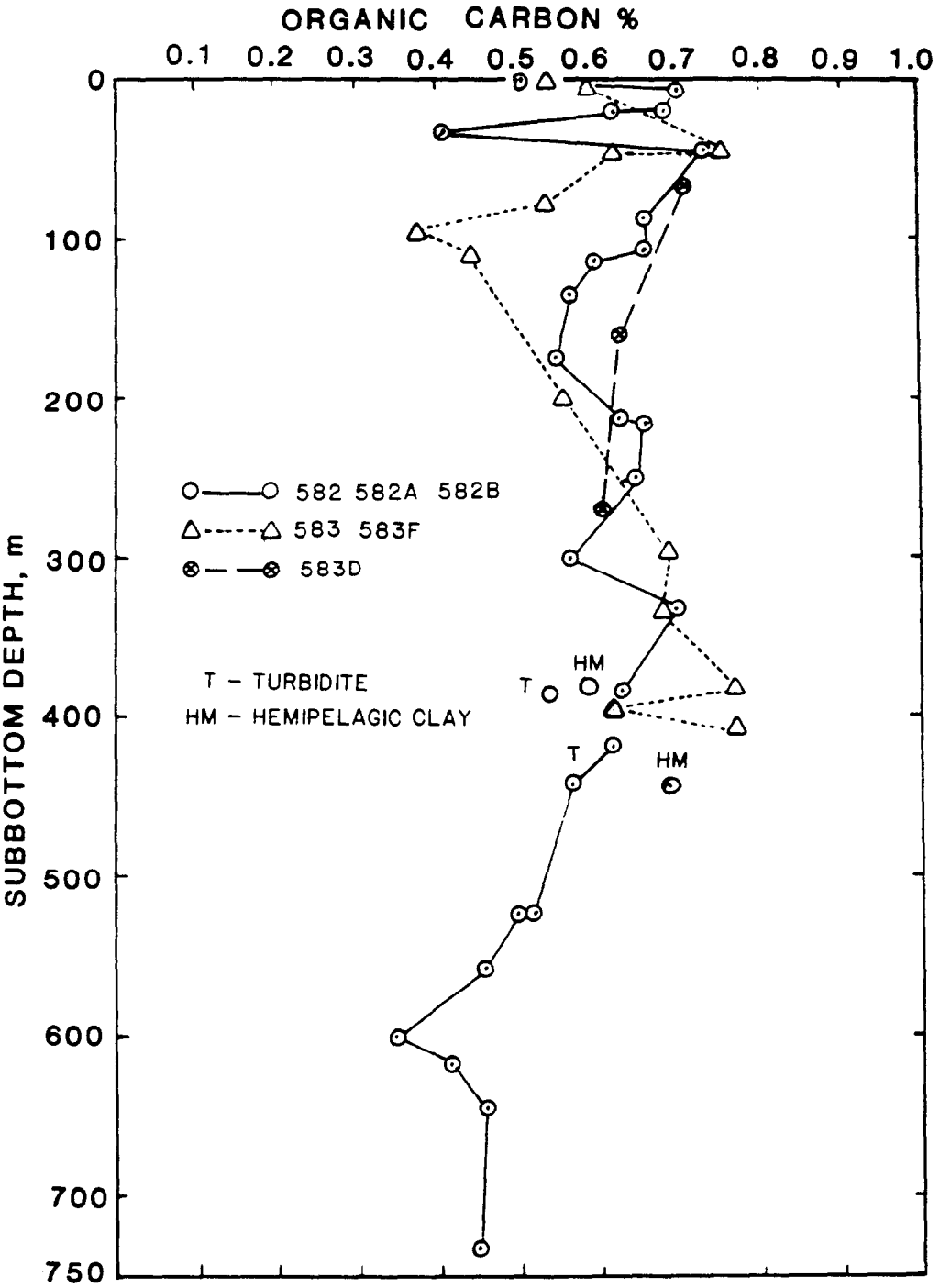

Figure 10. **COMPARISON OF TOTAL ORGANIC CARBON CONTENT OF SEDIMENTS FROM DSDP SITES 582 AND 583**
After Mukhopadhyay et al., 1986

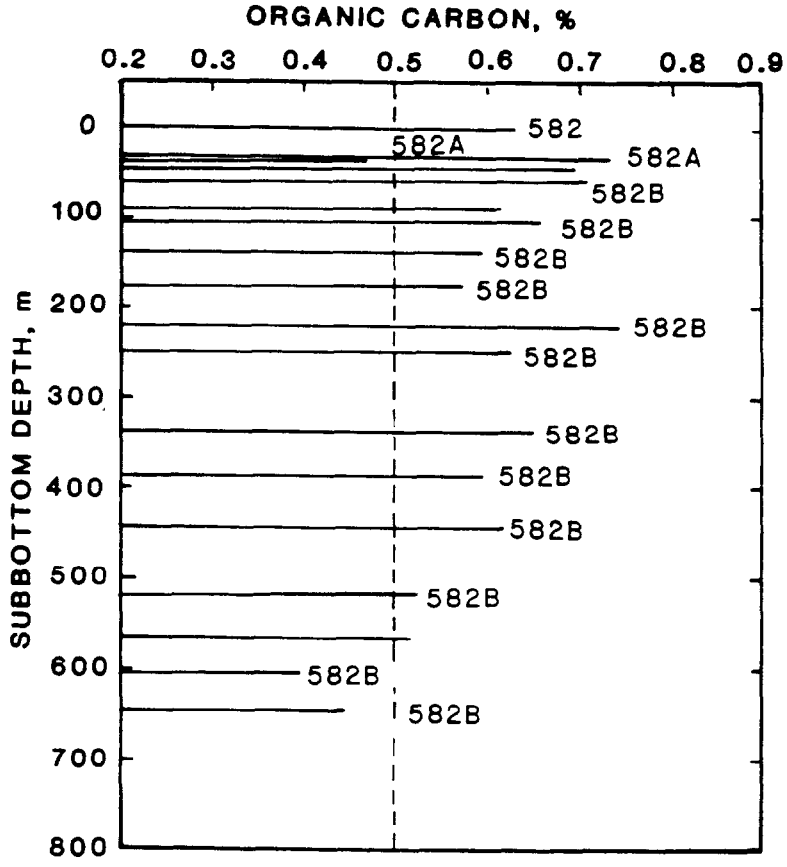

Figure 11. **TOTAL ORGANIC CARBON CONTENT IN SEDIMENTS FROM DSDP SITE 582**

After Kagami et al., 1986

accumulation is largely stimulated by downslope transportation processes. Furthermore, Mukhopadhyay et al. (1986) pointed out low TOC values at Sites 582 and 583, relative to other known turbidite sequences with rates of sedimentation similar to the high Nankai Trough rates. Consideration of the above presented data suggests that:

1. The production of in situ biogenic organic matter is particularly low in the lower continental slope of the Nankai Trough area.
2. A deep oxic environment as well as long distance of sediment transportation create unfavorable conditions for the preservation of the organic matter.
3. Low TOC values and significant uniformity in the lithological profiles of Sites 582 and 583 seem to be in agreement with the sedimentary pattern of the area, where the turbidites originated in fan delta systems of Tenryu, Ohi, Fuji and Kano rivers, transporting sediments to the Saruga Trough and further to the Nankai Trough area.
4. Although biogenic productivity in the middle and upper continental slope adjacent to the Nankai Trough is perhaps significantly elevated compared with the lower slope, the TOC values in the lower continental slope do not appear to be influenced by that fact.

Kerogen Composition

Examination of kerogen comprises a set of standard procedures which provide useful information in the evaluation process of hydrocarbon potential of source rocks. Except for previously presented analysis of organic matter, these procedures include the Rock-Eval pyrolysis technique first described by Espitalie et al. (1977), as well as a series of microscopic investigations. Both methods were applied in the process of investigation of the rock samples from Sites 582 and 583.

Rock-Eval Pyrolysis. The 100 mg powdered samples were heated up to 550°C at the programmed rate of 25°C/minute. The hydrocarbons already present in the analyzed sample are first released at temperatures below 300°C. These hydrocarbons, measured by a flame ionization detector (FID) are represented on a pyrogram as peak S_1. Further increase of heating temperature causes thermally generated hydrocarbons and hydrocarbon-like compounds to be volatized and measured by FID (peak S_2). The thermal hydrocarbon release is usually produced at temperatures between 300°C and 550°C. Eventually oxygen-containing elements, i.e. CO_2 and water, are measured by a thermal conductivity detector producing peak S_3.

Although the deepest sediments reached in the Nankai Trough have not been buried deeply enough for oil generation, the results from the pyrolysis elucidate some relationships with regard to their hydrocarbon potential. Two pyrograms of the whole-sediment samples from Site 582 are shown in Figure 12. The two analyzed rock samples were collected at 185-m and 256-m subbottom depths. Each pyrogram is composed of one S_1 peak and three S_2 peaks. The S_1 peaks show remarkably low values which represent a low amount of perhaps biogenically derived hydrocarbons. Occurrence of three S_2 peaks is indicative of

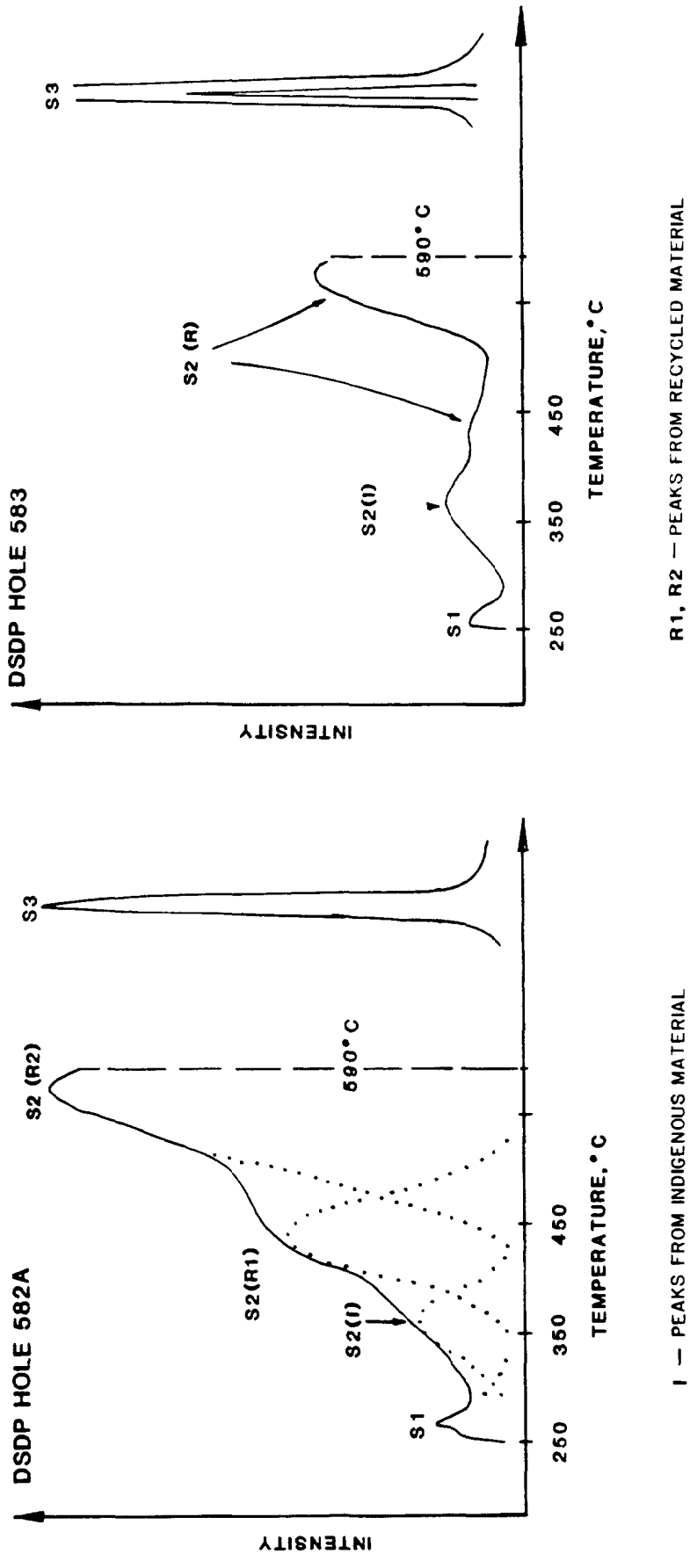

Figure 12. **PYROLYSIS RESULTS FROM DSDP SITES 582 AND 583**
After Sekiguchi and Hirai, 1986

kerogens of diverse origin. The first S_2 peaks generated at lower temperatures (up to 400°C) have been related to the indigenous kerogen (Kaichi and Hirai, 1986). The next S_2 peaks ($S_2(R_1)$ and $S_2(R_2)$), occurring at higher temperatures during pyrolysis, indicate the presence of recycled, matured and/or overmature kerogen. Similar conclusions can be drawn from a number of other pyrolysis data of rock samples shown in Table 3.

Kerogen type is commonly characterized by two standard indices: the hydrogen index (HI) defined as S_2/organic carbon and oxygen ratio (OI) calculated as S_3/organic carbon. Both indices are strongly dependent on elemental composition of kerogen and correlate well with hydrogen/carbon (H/C) and oxygen/carbon (O/C) ratios respectively. For the latter reason the two pairs of ratios can be used interchangeably. Using HI and OI values, a van Krevelen diagram (Tissot and Welte, 1984) can be constructed. This diagram delineates the areas of various paths of thermal evolution of kerogen, providing its useful classification based on an H/I and O/I relationship (Durand et al., 1972; Tissot and Welte, 1984). Various investigations showed that the evolution of kerogen is closely related to its environment of deposition, i.e. different hydrogen:oxygen ratios. Three types of kerogen have been distinguished on the basis of initial hydrogen carbon and oxygen contents and changes of their ratios as the kerogen evolved:

Type I kerogen has a high initial H/C ratio (1.5 or more) and relatively low O/C ratio (usually smaller than 0.1). It is rich in aliphatic structures, i.e. in hydrogen; some algal deposits produce this type of kerogen. During the process of pyrolysis in temperatures up to 550 to 600°C, Type I kerogen produces more volatile and extractable compounds than any other type of kerogen.

Type II kerogen indicates a marine depositional environment. It is characterized by relatively high H/C and O/C ratios ranging from 0.02 to 0.2. The organic matter is derived from a mixture of phytoplankton, zooplankton and microorganisms deposited in a reducing environment. This kerogen is a frequent constituent in many petroleum source rocks and oil shales.

Type III kerogen has a low initial H/C atomic ratio (less than 1.0) and high O/C ratio (often reaching values of 0.2 to 0.3). This type of kerogen is mainly derived from continental higher plants and vegetal debris. Despite the low H/C ratios, the possibility of oil generation from this kerogen is limited. Certain economic quantities of gas can be generated if it is buried sufficiently deep.

A Van Krevelen diagram, based on analyzed sediment samples from Sites 582 and 583, is shown in Figure 13. Because of the diversity of the kerogen in the samples and lack of organic carbon content for each peak S_2, integrated values of the total S_2 peak area had to be used. The data indicate that kerogen in the samples from Sites 582 and 583 are mainly of Type III (Tissot et al., 1974). High values of the oxygen index (O1) indicate that these kerogens were mostly oxidized during their transportation to depositional areas.

As was previously stated, another indicator which can be drawn from the Rock-Eval pyrolysis is genetic potential (GP) of kerogen. Genetic potential is defined as a sum of the values of peaks S_1 and S_2, expressed in mg HC per 1 g of

TABLE 3.
RESULTS OF PYROLYSIS OF WHOLE SEDIMENT SAMPLES FROM DSDP SITES 582 AND 583.
After Sekiguchi and Hirai, 1986.

Drilling Site	Subbottom depth m	Rock-Eval Pyrolysis* S_1	S_2	S_3
582A	0.00-5.22	0.11	5.54	1.36
582A	29.10-33.42	0.07	1.33	1.37
582A	58.20-61.44	0.06	0.48	3.45
582A	87.30-87.96	0.08	0.91	1.92
582A	116.10-118.63	0.09	0.52	2.11
582A	135.50-142.35	0.07	0.71	2.59
582A	183.60-187.24	0.06	0.77	2.54
582A	212.50-212.97	0.07	0.69	2.66
582A	231.90-232.82	0.06	0.72	2.72
582A	251.10-253.23	0.06	1.63	1.34
582A	279.90-280.53	0.07	0.21	2.14
582A	318.30-319.48	0.05	0.42	2.74
582A	337.50-338.91	0.05	0.26	2.33
582A	365.90-366.61	0.06	0.29	2.77
582A	394.30-394.74	0.05	0.35	2.07
582A	413.20-416.47	0.05	0.25	2.12
582A	432.00-434.50	0.05	0.74	2.97
582A	460.50-461.22	0.04	0.88	2.06
582A	498.60-499.76	0.05	1.05	2.45
582A	537.00-538.79	0.04	0.46	2.15
582A	566.00-568.15	0.03	1.31	1.02
582A	604.50-606.61	0.03	0.93	1.20
582A	623.70-624.18	0.03	0.47	2.23
582A	642.90-643.75	0.04	0.32	2.60
582A	671.80-675.22	0.04	1.11	1.34
582A	691.20-692.67	0.03	1.54	1.18
582A	710.60-712.61	0.04	0.67	2.02
583B	5.00-8.25	0.08	1.20	2.60
583C	20.00-22.16	0.08	0.63	1.87
583C	40.00-40.46	0.05	0.77	2.25
583C	66.00-67.78	0.08	0.55	3.70
583D	95.00-97.16	0.06	0.39	2.14
583D	123.70-126.32	0.08	0.83	2.97
583D	152.60-153.98	0.06	0.71	3.36
583D	181.70-182.13	0.05	0.42	2.65
583D	220.20-221.46	0.07	2.41	1.38
583D	249.30-251.06	0.06	0.39	2.76
583D	268.70-274.13	0.06	0.63	2.52
583D	316.9-318.63	0.05	0.91	3.10

* mg of hydrocarbon per 1 g of sample

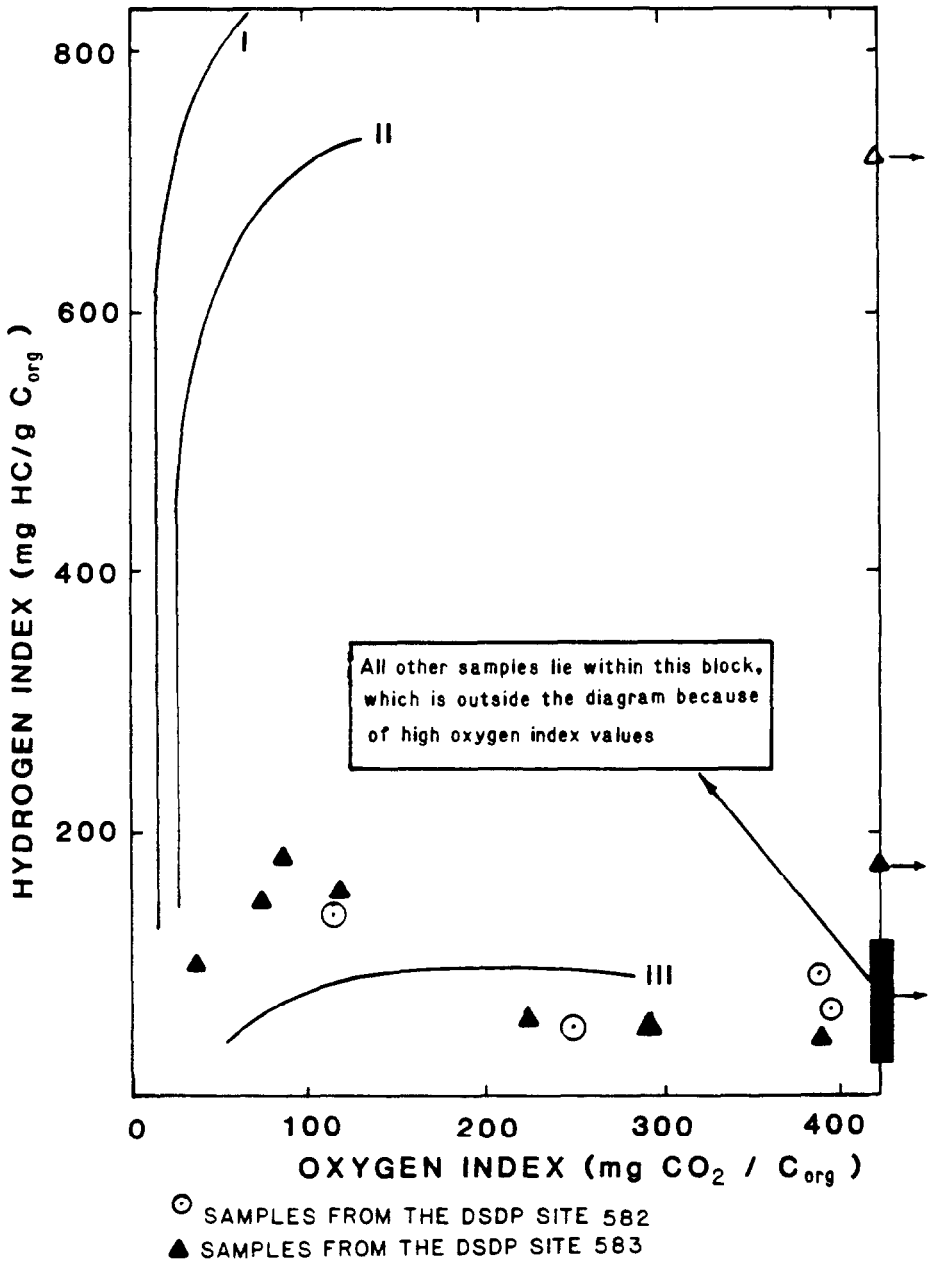

Figure 13. **MODIFIED VAN KREVELEN DIAGRAMS FROM DSDP SITES 582 and 583**
After Mukhopadhyay et al, 1986

sample. For most samples, GP values were found below 2.5 mg HC/g sample, indicating very low potential for hydrocarbons (Figure 11).

The organic matter in sedimentary profiles of Sites 582 and 583 was also analyzed for maceral composition (Table 4). Visual kerogen examinations of the samples revealed that amorphous debris ranging from 66 to 90% are major constituents, while woody-coaly elements occur in subordinate quantities (Figure 14; Table 4). Rock-Eval pyrolysis confirmed other independently obtained results that the analyzed kerogens are not sapropelic of marine origin. Optical microscopic examination of the kerogens concluded that most (i.e. 80 to 90%) is of terrestrial origin. The kerogens were found to include macerals of huminite/vitrinite, inertinite, sporinite, cutinite, and resinite or suberinite. The analyses of maceral composition of the organic matter in the Nankai Trough further confirm that the encountered kerogen is type III and type II-III.

Thermal Maturity

Vitrinite reflectance (R_o) and the temperature (T_{2max}) at which the maximum hydrocarbons are released during pyrolysis are commonly accepted as reliable indicators of kerogen thermal maturity. Reflectance measurements which were originally used in evaluation of coal, have been subsequently applied to particles of disseminated kerogen in shales and other rocks (Vassoevich et al., 1969; Dow, 1977). Three stages of hydrocarbon source rock maturation have been established on the basis of vitrinite reflectance values (Tissot and Welte, 1984):

- $0.5 < R_o < 0.7\%$--early stage of diagenesis at which source rock is immature for hydrocarbon generation
- $0.7 < R_o < 2\%$--catagenesis stage. These values of R_o usually correspond with a main zone of oil generation (the oil window)
- $R_o > 2\%$ characterizes hydrocarbon source rocks where methane is the principal hydrocarbon product.

The evaluation of thermal maturity of the sediments in the profiles of Sites 582 and 583 was based on mean values of vitrinite-huminite reflectance. The temperature from pyrolysis (T_{2max}) could not be applied due to the previously discussed nature of the pyrograms. Some reflectance (R_o) data from the Nankai Trough are shown in Table 5.

The analyses of the kerogen reflectance confirmed the presence of indigenous as well as allochtonous kerogen (Figure 15). The lower values of R_o in analyzed samples were attributed to indigenous kerogen while the higher values most likely represent more mature recycled kerogen from older rocks. Data in Figure 15 and Table 5 indicate that most of the analyzed indigenous kerogen has an R_o value around 0.2% which qualifies the sediments as immature with respect to hydrocarbon potential. At the present time it is not possible to construct a credible kerogen maturation trend based on available data in the Nankai Trough. However, the average trend of low values R_o from Site 582 is correct, the oil generation threshold probably lies at 1,900 m subbottom depth. Although the maximum temperatures (T_{2max}) for S_2 peaks of pyrolyses (Table 6) cannot be considered as

TABLE 4

MACERAL COMPOSITION OF ORGANIC MATTER IN SEDIMENTS AT DSDP SITES 582 AND 583*
After Mukhopadhyay et al., 1986.

Drilling Site	Subbottom Depth m	Huminite/ Vitrinite	Inertinite	Amorphous Humic Matter	Particulate Liptinite B	Particulate Liptinite A	Alginite	Amorphous Liptinite	Solid Bitumen
582	6.70	50	35		9	2	4		
582	23.40	52	20		5	4	19		
582B	114.20	69	15		8		7		
582B	212.85	62	18		12	2	6		
582B	300.80	48	29	1	13	3	6		
582B	416.68	43	29		21	3	4		
582B	523.26	49	30		12	2	3		
582B	616.76	52	22		11 (mainly resinite & cutinite)		4	2	9
582B	731.11	40	26	3	16 (mainly resinite)	4	9		2
583	0.75	35	30	2	18	6	9		
583	11.66	48	30	1	3	4	7	4	
583	47.70	58	29		8	1	4		
583	108.97	52	30		6	1	11		
583F	201.10	58	30		10				2
583F	295.66	40	42		4	5	8		1
583F	394.82	50	25		12		10		3
583D	67.00	29	50	2	11	1	7		
583D	163.37	58	25		5	4	8		
583D	269.77	50	22		18 (3% resinite)	4	6		

* All values are in vol % of maceral composition.

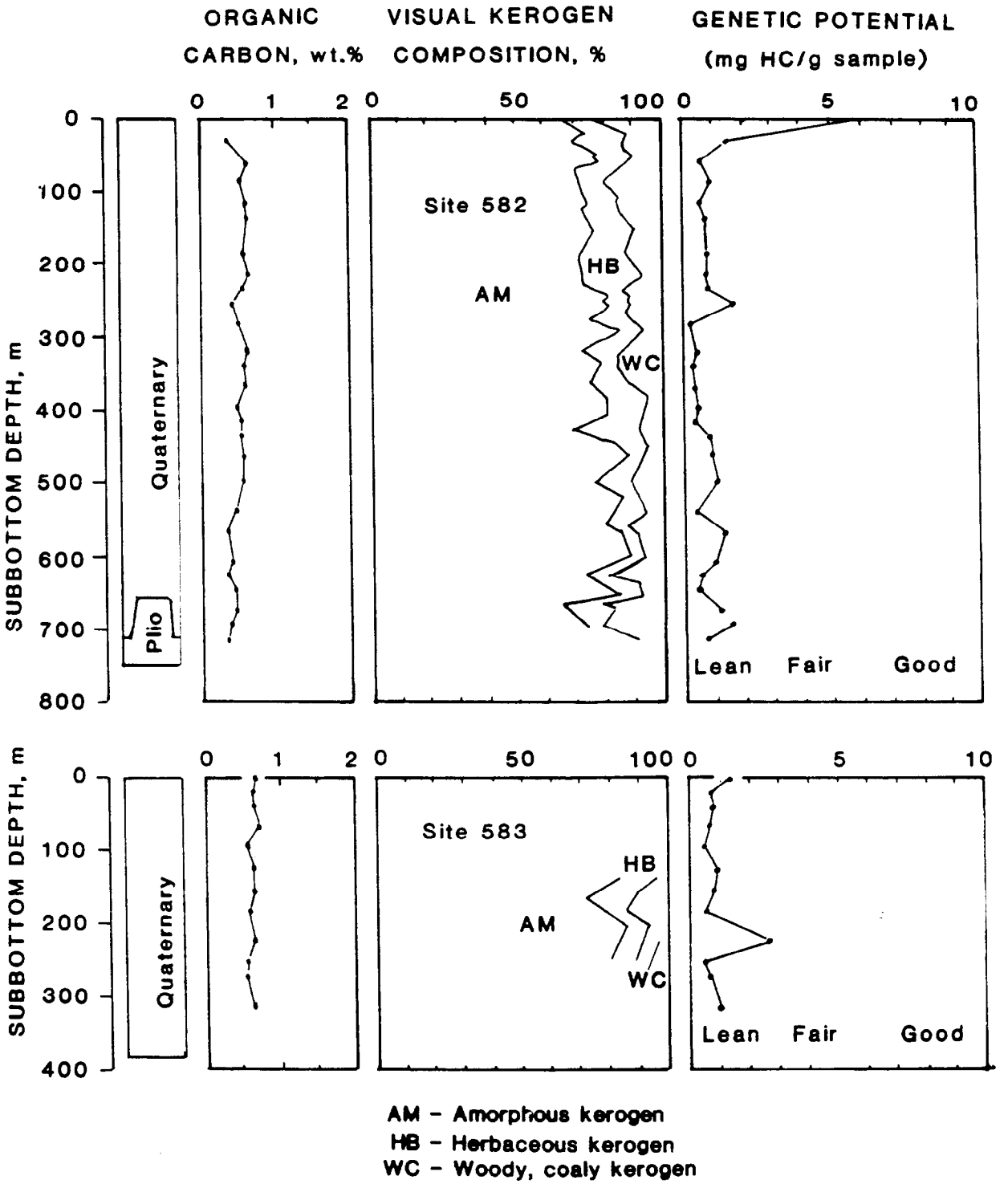

Figure 14. DISTRIBUTION OF ORGANIC CARBON, VISUAL KEROGEN AND HYDROCARBON GENETIC POTENTIAL IN SEDIMENTS OF DSDP SITES 582 AND 583 IN NANKAI TROUGH

After Sekiguchi and Hirai, 1986

TABLE 5.

KEROGEN REFLECTANCE OF SEDIMENTS AT DSDP SITES 582 AND 583.
After Sekiguchi and Hirai, 1986

Drilling Site	Subbottom Depth m	Number of Observations	Mean Reflectance %	Standard Deviation	Remarks
582A	29.10-33.42	14	0.215	0.038	
		24	0.412	0.066	Inertinite
582A	154.80-156.06	61	0.193	0.027	
		5	0.386	0.029	Inertinite
582A	183.60-187.24	5	0.172	0.016	
582A	212.50-212.97	19	0.197	0.025	
582A	337.50-338.91	63	0.251	0.039	
		57	0.341	0.054	Inertinite
	498.60-499.76	21	0.244	0.013	
583	55.40-59.61	12	0.210	0.014	
		2	0.345	0.035	Inertinite
583D	162.30-163.22	1	0.20		
583D	181.70-182.13	2	0.200	0.028	
583F	275.70-277.68	83	0.218	0.027	
		2	0.695	0.021	R V
		2	1.22	0.057	R V
		10	0.420	0.055	Inertinite
583G	442.00-443.39	4	0.180	0.008	

R V = Recycled vitrinite

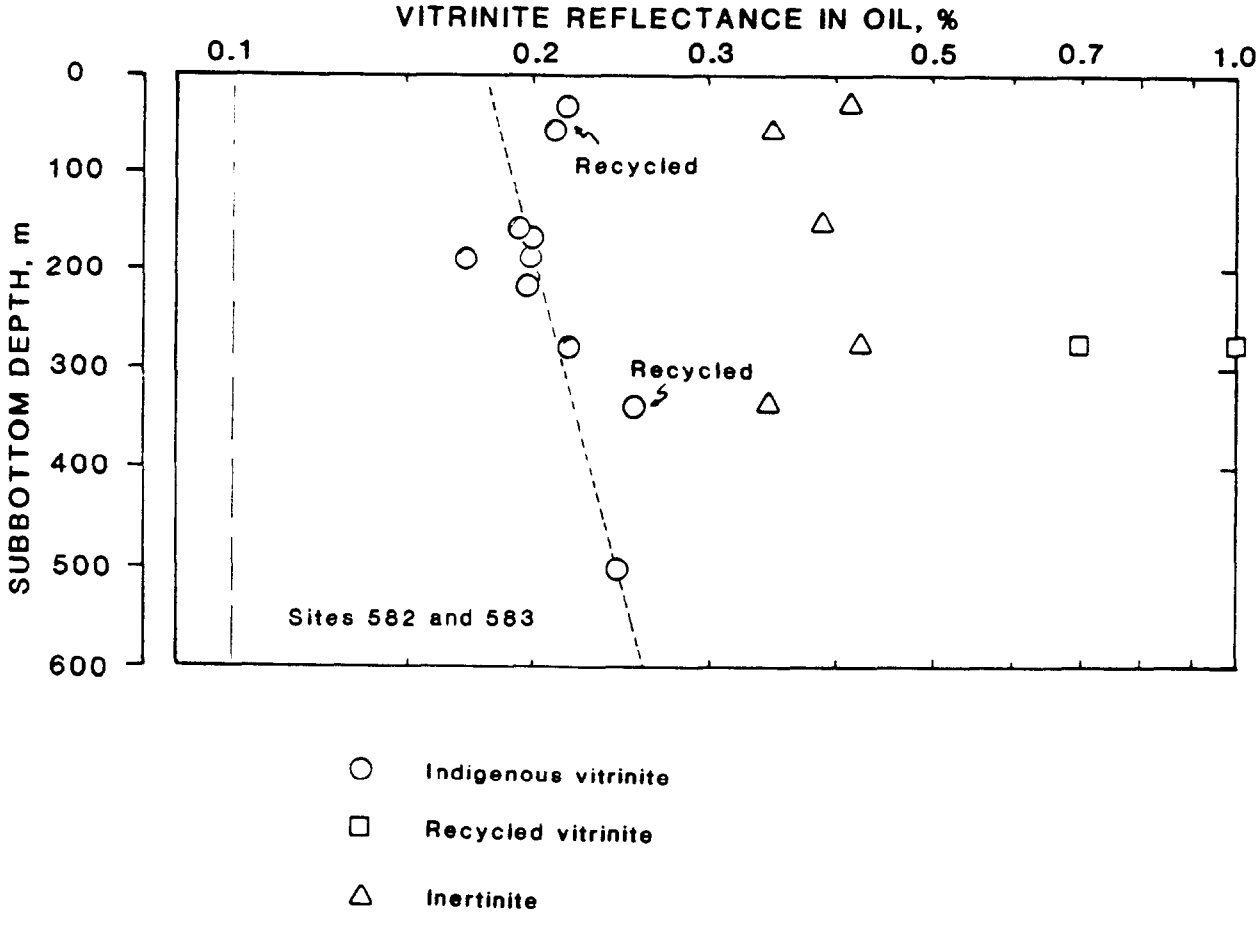

Figure 15. **VITRINITE REFLECTANCE FROM DSDP SITES 582 AND 583.**
After Sekiguchi and Hirai, 1986

TABLE 6.

HYDROGEN AND OXYGEN INDICES AND T_{max} OF SEDIMENT SAMPLES FROM DSDP SITES 582 AND 583. After Sekiguchi and Hirai, 1986.

Drilling Site	Subbottom Depth m	Hydrogen Index mg HC/g C_{org}	Oxygen Index mg CO_2/g C_{org}	T_{max} * I	T_{max} * R_1+R_2
82A	0.000-5.22	971	239		550
582A	29.10-33.42	350	361		550
582A	58.20-61.44	71	504	444	550
582A	87.30-87.96	160	337	451	550
582A	116.10-118.63	80	325	441	550
582A	135.50-142.35	106	387	447	550
582A	183.60-187.24	133	438	369	550
582A	212.50-212.97	103	397	461	550
582A	231.90-232.82	126	461		550
582A	251.10-253.23	388	319		550
582A	279.90-280.53	41	420		550
582A	318.30-319.48	65	422	451	550
582A	337.50-338.91	44	395	467	550
582A	365.90-366.61	48	462	445	550
582A	394.30-394.74	71	422	454	550
582A	413.20-416.47	45	385	445	550
582A	432.00-434.50	132	530	430	550
582A	460.50-461.22	152	355		550
582A	498.60-499.76	184	430	456	550
582A	537.00-538.79	98	457	468	550
582A	566.00-568.15	374	291		550
582A	604.50-606.61	233	300	460	550
582A	623.70-624.18	134	637	447	550
582A	642.90-643.75	70	565	442	550
582A	671.80-675.22	241	291		550
582A	691.20-692.67	395	303	474	550
582A	710.60-712.61	186	561	405	550
583B	5.00-8.25	176	382	456	550
583C	20.00-22.16	103	307		550
583C	40.00-40.46	115	336	447	550
583C	66.00-67.78	74	500	415	550
583D	95.00-97.16	71	389	454	550
583D	123.70-126.32	128	457	442	550
583D	152.60-153.98	108	509	442	550
583D	181.70-182.13	71	449	451	550
583D	220.20-221.46	371	212	450	550
583D	249.30-251.06	71	502	441	550
583D	268.70-274.13	119	475	445	550
583D	316.90-318.63	142	484	437	550

* I - indigenous kerogen, R_1+R_2 - recycled kerogen

fully reliable, their relatively low values seem to be supportive of the conclusions of low thermal maturity of the upper sedimentary sequence in the Nankai Trough.

Hydrocarbon Gases

The number and extent of gas analyses from sediments in the Nankai Trough is not adequate for their full geochemical evaluation, yet some useful preliminary conclusions can be drawn.

Hydrocarbon gases with minor amounts of CO_2 and traces of H_2S were found to be present in the form of gas pockets at Sites 582 and 583 in the Nankai Trough. Because of the anticipated presence of gas hydrates prior to drilling these holes, the gas logging program was carefully executed. From the listed gas logging data (Tables 7, 8, 9 and 10), it can be readily observed that methane is a major hydrocarbon component and constitutes up to 95% of the detected and directly directly measured gases. The values of C_1 from vacutainer are lower as a result of the procedure where the in situ gas mixture is diluted by atmospheric air. The methane/ethane ratio was introduced by Bernard et al. (1976) as a good indicator of biogenic or thermogenic origin of hydrocarbons. According to these authors, values of C_1/C_2 greater than 1,000 can be attributed to the hydrocarbons of biogenic provenance, whereas values smaller than 50 are indicative of thermogenic hydrocarbons. Chromatographic data from Sites 582 and 583 revealed C_1/C_2 values ranging from 21,000 to 735,000 (Tables 7 and 9; Figures 16, 17 and 18).

Biogenic provenance of hydrocarbon gases in the sediments of Nankai Trough was further ascertained from isotopic analyses of methane in samples collected at subbottom depths of 12 m (Site 583), 256.5 m (Site 583F), 318 m (Site 583F), 372.5 m (Site 583F) and 501.5 m (Site 583F). The ^{13}C values for the analyzed samples ranged from -73.5 per mil to -66 per mil. The omnipresence of CO_2 provides an additional indication that the detected hydrocarbon gases were generated through bacterial degradation of organic matter.

TABLE 7.
COMPOSITION OF SEDIMENT GASES FROM DSDP SITE 582.
After Kagami et al., 1986.

Subbottom Depth	Methane (C_1 in vol. %)	Ethane (C_2 in ppm)	C_1/C_2 ($\times 10^{-3}$)	CO_2 (%)
9.7	6.54	3.11	21.00	0.18
28.5	68.4	4.79	143.00	1.23
10	23.6	1.54	148.40	0.35
45	84.1	2.56	328.50	1.14
62	86.2	2.68	373.20	1.38
72	86.0	2.78	369.10	1.14
90.4	84.3	2.02	417.30	1.10
114	90.8	1.76	515.90	0.79
130	73.7	1.47	501.40	0.83
180	90.7	2.48	365.70	1.32
186.6	84.3	2.45	344.10	1.70
196.2	66.7	5.81	114.80	0.40
218.5	18.6	8.16	22.79	0.35
228.2	85.7	3.97	215.90	2.12
237.9	86.6	12.2	71.22	0.41
243.5	87.2	3.87	225.30	0.84
258.6	76.4	4.20	181.90	0.81
267.3	90.9	4.40	206.60	0.48
288.3	90.6	5.37	168.70	0.77
334.9	87.5	9.03	96.90	0.74
339.0	82.0	6.51	126.00	0.63
350.1	83.8	10.4	54.40	0.47
362.2	79.1	10.2	77.70	1.08
394.1	59.4	16.2	36.64	1.20
397.3	61.7	13.4	45.98	0.93
405.2	84.2	13.3	63.31	1.06
416.1	85.8	13.4	62.63	1.13
424	66.8	11.3	59.12	1.09
433.5	81.9	12.8	63.79	1.64
455.5	87.0	12.3	70.73	1.17
462	82.9	12.	69.19	1.74
500.2	46.4	6.66	69.67	0.47
520.8	84.5	13.3	63.53	1.96
540.1	9.57	1.9	50.37	0.39
559.3	73.9	12.7	57.87	1.67
572.3	57.1	10.2	55.94	1.35
591.4	67.1	10.7	63.27	1.61
601.5	29.	4.78	56.52	0.83
607.8	2.86	2.35	12.17	0.34
617.2	16.4	4.0	41.00	0.46
626.7	1.7	0.5	34.00	0.26
639.3	1.05	0.23	46.10	0.35
649.9	3.15	0.64	49.07	0.48
658.5	0.01	Tr.		0.15
676.2	4.47	Tr.		0.50
721.4	0.00	Tr.		0.18

TABLE 8.

COMPOSITION OF SEDIMENT GASES FROM DSDP SITE 582. After Kagami, 1986.

DSDP Hole	Subbottom depth, m	Ethane ppm	Propane ppm	Isobutane ppm	Butane ppm	Neopentane ppm	Isopentane ppm	Pentane ppm
582	9.7	1.67	N.D.*					
	28.5	3.35	N.D.					
582A	10.2	1.59	Tr.**	N.D.				
	45.3	2.56	0.926	N.D.				
582B	62.6	2.68	1.65	N.D.				
	72.3	2.79	1.58	Tr.	N.D.			
	90.4	2.02	1.38	Tr.	N.D.			
	114.5	1.76	1.68	Tr.	N.D.			
	130.2	1.47	1.35	Tr.	N.D.			
	180.6	2.48	2.85	Tr.	N.D.			
	186.6	2.45	2.39	Tr.	N.D.			
	196.2	5.81	1.67	0.33	0.27	N.D.		
	218.5	8.16	1.84	2.13	1.86	0.93	Tr.	0.80
	228.2	3.97	3.46	0.69	N.D.	N.D.	N.D.	N.D.
582B	237.9	12.2	1.47	0.21	N.D.			
	243.5	3.87	3.04	0.43	N.D.			
	258.6	4.20	2.38	0.60	N.D.			
	267.3	4.40	2.60	0.88	N.D.	N.D.	Tr.	N.D.
	288.3	5.37	3.30	0.83	N.D.	N.D.	0.41	N.D.
	334.9	9.03	3.10	1.03	N.D.	N.D.	0.52	N.D.
	339.0	6.51	4.44	1.11	N.D.	N.D.	1.10	N.D.
	350.1	15.4	3.21	0.64	N.D.	N.D.	0.77	N.D.
	362.2	10.2	5.19	1.30	0.43	0.21	1.31	Tr.
	394.1	16.2	4.14	1.38	N.D.	N.D.	1.38	N.D.
	397.3	13.4	4.63	1.54	N.D.	N.D.	0.80	N.D.
	405.2	13.3	4.58	1.15	N.D.	N.D.	0.38	N.D.
	416.1	13.4	5.11	1.02	N.D.	N.D.	1.00	N.D.
	424	11.3	4.60	1.15	N.D.	N.D.	0.23	N.D.
	433.5	12.8	6.34	2.10	N.D.	N.D.	0.30	N.D.
	455.5	12.3	6.25	2.10	Tr.	0.26	0.05	N.D.
	462	12.0	5.79	2.00	0.40	Tr.	3.00	N.D.
	500.2	6.66	2.87	0.96	N.D.	N.D.	Tr.	N.D.
	520.8	13.3	5.03	0.84	N.D.	N.D.	N.D.	N.D.
	540.1	1.90	0.95	N.D.				
	559.3	12.7	3.77	0.90	N.D.			
	572.3	10.2	3.40	0.85	N.D.			
	591.4	10.7	3.65	1.04	N.D.			
	601.5	4.78	1.77	0.59	N.D.	0.29	0.30	N.D.
	607.8	2.35	1.56	Tr.	Tr.	N.D.		
	617.2	4.00	2.67	0.67	0.89	N.D.		
	626.7	0.50	Tr.	Tr.	N.D.			
	639.3	0.23	N.D.					
	649.9	0.64	0.50	N.D.				
	658.6	N.D.						
	676.2	Tr.	N.D.					
	721.4	Tr.	N.D.					

* Traces (Tr): < 0.02 ppm
** Not detected (N.D.): < 0.01 ppm

TABLE 9.

COMPOSITION OF SEDIMENT GASES FROM DSDP SITE 583.
After Kagami et al., 1986.

DSDP Hole	Subbottom Depth m	Sampling Method	Methane vol.%	C_1/C_2 $x10^{-3}$	CO_2 %
	10.2	Vacutainer	73.45	253.300	0.72
	19.5	Vacutainer	70.91	270.600	1.11
	21.1	Vacutainer	63.44	360.500	1.77
	38.6	Vacutainer	72.10	397.400	1.13
	50.2	Vacutainer	67.04	392.400	1.16
583	57.8	Vacutainer	55.07	432.200	0.93
	60.2	Vacutainer	30.12	101.500	0.12
	75.3	Vacutainer	32.95	116.400	0.17
	92.5	Vacutainer	45.34	362.700	0.33
	100.2	Vacutainer	48.97	362.700	0.94
	111.6	Vacutainer	65.16	513.100	1.21
	118.8	Vacutainer	60.73	530.600	1.98
	125.2	Vacutainer	62.08	395.400	1.08
	140.1	Vacutainer	56.64	207.100	0.51
	10.2	Vacutainer	62.99	346.100	0.634
	18.5	Vacutainer	68.35	427.200	0.804
	19.7	Vacutainer	70.12	547.800	1.02
583A	20.4	Vacutainer	65.00	625.000	1.00
	21.2	Vacutainer	66.95	619.900	0.755
	22.3	Vacutainer	64.72	492.900	1.10
	30.8	Vacutainer	70.76	735.800	0.692
	40.6	Vacutainer	62.34	167.600	0.998
	47.2	Vacutainer	70.57	664.900	0.950
	50.2	Vacutainer	57.45	407.446	2.342
	8.4	Vacutainer	66.65	396.600	1.359
583B	12.8	Vacutainer	74.03	417.900	1.241
	19.3	Vacutainer	76.78	673.500	0.934
583C	27.2	Vacutainer	70.45	448.700	1.07
	39.3	Vacutainer	57.06	538.300	0.864
	15.8	Vacutainer	48.75	455.600	1.65
	96.2	Vacutainer	63.50	466.900	1.34
	108.3	Vacutainer	36.10	229.600	0.87
583D	121.4	Vacutainer	58.64	333.200	1.42
	125.2	Vacutainer	68.92	133.000	0.76
	136.2	Vacutainer	50.09	218.700	1.10
	145.5	Vacutainer	47.16	354.600	1.14

TABLE 9 (cont'd).

DSDP Hole	Subbottom Depth m	Sampling Method	Methane vol.%	C_1/C_2 x10^{-3}	CO_2 %
583D	151.5	Direct	94.05	427.500	1.58
	151.5	Vacutainer	60.58	275.400	1.39
	170.8	Direct	87.83	675.600	1.69
	170.8	Vacutainer	37.63	287.200	1.15
	175.2	Direct	91.68	377.300	1.38
	175.2	Vacutainer	65.22	268.400	0.99
	182.5	Vacutainer	63.07	123.400	1.06
	195.8	Vacutainer	57.49	112.900	1.44
	208.1	Vacutainer	61.78	172.600	0.87
583D	223.5	Direct	89.93	228.500	2.02
	230.2	Direct	23.72	539.100	0.39
	249.4	Direct	96.36	319.100	1.16
	258.2	Direct	94.95	404.000	0.97
	258.2	Vacutainer	54.52	232.000	0.69
	270.1	Direct	93.67	255.200	0.001
	270.1	Vacutainer	74.48	202.900	0.61
	279.4	Direct	83.99	171.200	1.06
	318.8	Direct	96.60	185.800	0.40
	318.8	Vacutainer	60.10	241.400	0.83
	192.3	Vacutainer	76.01	212.900	0.884
	257.2	Direct	96.17	182.500	0.440
	257.2	Vacutainer	70.18	133.200	0.334
	268.5	Direct	8.13	165.900	0.143
	268.5	Vacutainer	9.33	189.200	0.098
	275.7	Direct	87.72	261.900	0.854
	275.7	Vacutainer	80.35	239.900	0.349
583F	298.3	Direct	93.02	155.200	0.392
	298.3	Vacutainer	78.51	130.900	0.380
	304.4	Direct	78.46	75.930	0.760
	315.4	Vacutainer	84.75	141.700	0.504
	325.4	Direct	59.08	113.600	1.013
	325.4	Vacutainer	68.75	132.200	0.931
	331.2	Direct	94.79	62.360	0.333
	331.2	Vacutainer	28.57	53.500	0.235
	370.3	Direct	89.52	68.340	0.314
	382.5	Direct	88.72	96.960	0.930
	395.3	Direct	95.55	71.250	0.605
	395.3	Vacutainer	84.14	62.800	0.483
	400.8	Direct	93.96	22.570	0.218
	400.8	Vacutainer	87.79	21.100	0.272
	423.2	Vacutainer	28.02	33.042	0.158

TABLE 10.

COMPOSITION OF HYDROCARBON GASES FROM DSDP SITE 583

After Kagami, 1986.

DSDP Hole	Subbottom Depth, m	Ethane ppm	Propane ppm	Isobutane ppm	Butane ppm	Neopentane ppm	Isopentane ppm	Pentane ppm
	10.2	2.90	3.33	N.D.				
	19.5	2.62	2.64	0.29	N.D.	N.D.	N.D	N.D.
	21.1	1.76	3.04	0.45				
	38.6	1.81	2.86	0.29				
583	50.2	1.80	3.92	0.30				
	57.8	1.28	2.63	0.22				
	60.2	2.97	1.20	0.22				
	75.3	2.83	0.52	Trace				
	92.5	1.25	1.82	0.11				
	100.2	1.35	2.02	0.12				
	111.6	1.27	2.08	0.20				
	118.8	1.14	2.57	0.20				
	125.2	1.57	1.40	0.10				
	140.1	2.73	1.30	Trace				
	10.2	1.82	3.52	0.67	2.36	N.D.	N.D.	2.35
	18.5	1.60	3.03	0.45	0.59			0.97
	19.7	1.28	2.26	0.36	0.36			0.96
	20.4	1.04	1.90	0.34	0.56			0.49
583A	21.2	1.08	2.00	0.22	0.18			0.21
	22.3	1.31	2.04	0.25	Trace			0.17
	30.8	0.96	2.38	0.16				Trace
	40.6	3.72	1.54	0.11				
	47.2	1.06	2.10	0.16				Trace
	50.2	1.41	2.37	0.31	Trace			Trace
	8.4	1.72	1.73	0.17				
	12.8	1.98	1.68	0.13				
583B	19.3	1.77	1.83	0.17				
	30.5	1.14	1.88	0.11				
	27.2	1.57	1.97	0.13				
583C	39.3	1.06	1.69	0.10				
	15.8	1.07	2.33	0.18	N.D.	N.D.	N.D.	N.D.
	96.2	1.36	2.15	0.21				
	108.3	1.57	1.74	0.21				
	121.4	1.76	2.67	0.40				
	125.2	5.18	1.90	0.38				
	136.2	2.29	2.08	0.36			Trace	
	145.5	1.33	1.68	0.34			0.14	
583D	151.5	2.20	4.36	0.62			0.27	
	170.8	1.31	1.86	0.38			0.15	
	175.2	2.43	2.44	0.29				
	182.5	5.11	4.47	0.71			0.18	
	195.8	5.10	6.02	1.23	Trace	Trace	0.36	
	208.1	3.58	7.38	1.21	Trace	Trace	0.36	
	223.5	3.93	6.57	0.81			0.11	
	230.2	0.44	0.62					
	249.4	3.02	4.37	0.75			0.18	
	258.2	2.35	3.78	0.71			0.45	
	270.1	3.67	5.49	0.78			0.27	
	279.4	4.91	6.54	0.43		Trace	0.36	
	318.8	5.20	4.30	0.41			Trace	
	192.3	3.57	5.20	0.20	N.D.	N.D.	N.D.	N.D.
	257.2	5.27	4.90	0.42				
	268.5	0.49	0.67					
	275.7	3.35	5.60	0.63				
	298.3	6.00	5.10	0.51				
	304.4	10.33	5.03	0.60			0.17	
583F	315.4	5.98	7.25	0.86	Trace		0.10	
	325.4	5.20	8.62	1.87	0.18		0.20	
	331.2	15.20	4.04	0.20			Trace	
	370.3	13.1	2.04	0.15			Trace	
	382.8	9.15	11.80	3.35	0.36	0.17	0.53	
	395.3	13.4	7.27	2.04	0.32	0.13	0.90	
	400.8	41.6	3.21	0.36			0.33	
	423.2	8.48	2.32	0.47	0.34		0.33	

*N.D.: not detected, <0.1 ppm

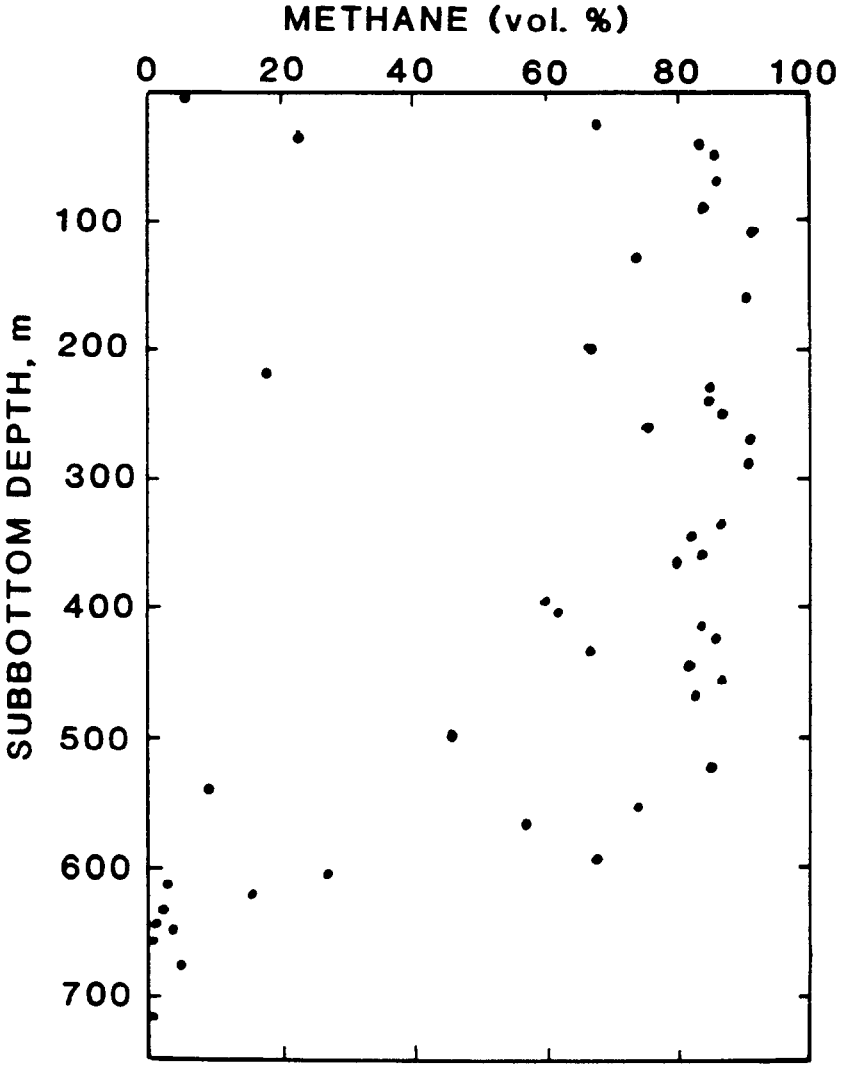

Figure 16. **METHANE CONTENT OF CORE GASES FROM DSDP SITE 582**
After Kagami et al., 1986

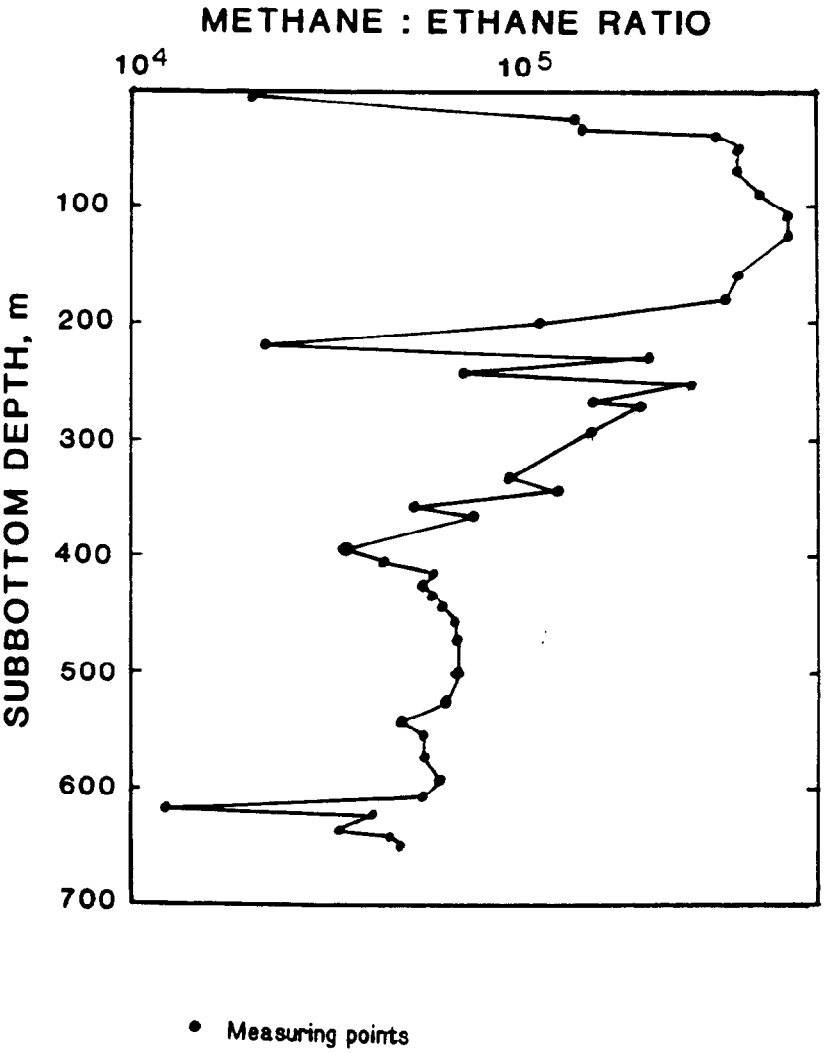

Figure 17. **RATIO OF METHANE TO ETHANE IN CORE GASES FROM DSDP SITE 582.**
After Kagami et al., 1986

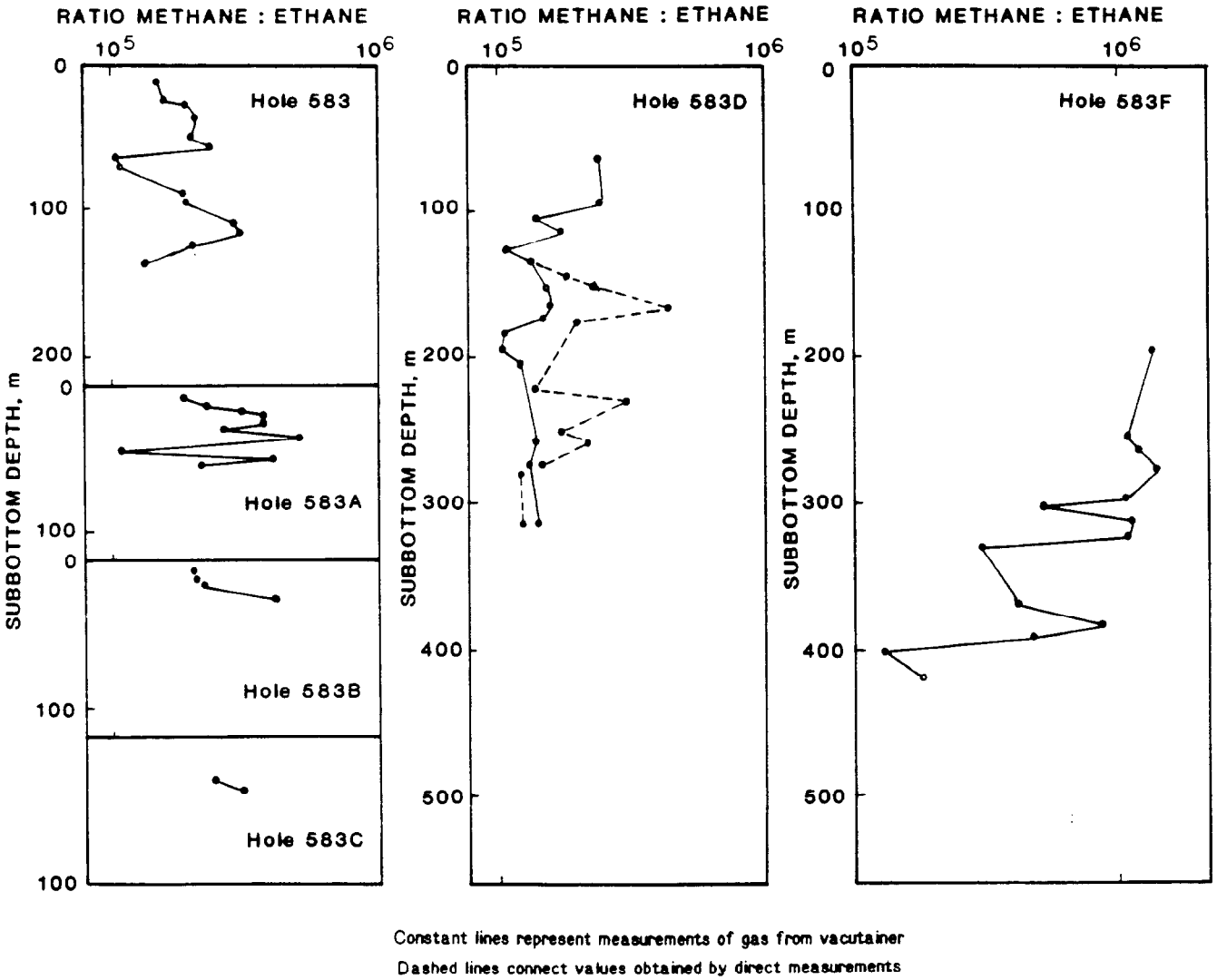

Figure 18. **RATIOS OF METHANE TO ETHANE IN CORE GASES FROM DSDP SITE 583**

After Kagami et al., 1986

PART II

FORMATION AND STABILITY OF GAS HYDRATES

The Nankai Trough is a convergent margin with seismic evidence of gas hydrate presence. Although the term "trough" suggests the central part of an elongate depression in the sea floor, the seismic evidence of gas hydrates was identified from the middle to lower continental slope landward of the Trough itself. Investigation of the tectonic history of the Nankai Trough governed the choice of the DSDP drilling sites in the area. Better seismic resolution of the outermost accretionary wedge of the Nankai Trough favored drilling on the lowermost continental slope. The DSDP holes within the Nankai Trough study region were drilled with great caution due to possible gas hydrate presence. No boreholes have been drilled in the continental slope sections where the most prominent bottom simulating reflectors occur. Thus few drilling data on the sediments near the BSRs are available. Data from distant drillholes must be used to infer the subsurface conditions of the areas of most interest for gas hydrate study.

No gas hydrates were found in cores from Sites 298 and 583. Prior to drilling, speculation on gas hydrates had centered on the possible role of faults as pathways for migrating hydrocarbons. Data on some factors crucial for evaluation of gas hydrates in the areas of the Nankai Trough study regions with documented BSRs are absent. We have made efforts to pinpoint these data gaps as well as points of contention in prior interpretation of gas hydrate occurrence of the study region.

Among the principal factors which control the presence of gas hydrates are: sedimentary environment(s), availability of hydrocarbon gas, geothermal gradient, and pressure gradients.

Sedimentary Environments

The role of sedimentary environment in formation and subsequent stabilization of natural gas hydrates is quite complex in most cases. Many important aspects of the role are poorly known; multidisciplinary efforts are in progress to resolve them. Four aspects of sedimentary environments seem to be particularly important to gas hydrate formation:

1. sediments as hydrocarbon source rocks
2. reservoir characteristics of sediments for hydrocarbon gases and for gas hydrates
3. sedimentation rates and erosional processes
4. geothermal processes related to sediment type

Sediments of the Nankai Trough and their potential for hydrocarbon generation were discussed at length in Part I of this report. Although the discussion was based on the data from the lowermost continental slope (DSDP Sites 582, 583), the data are generally applicable to the adjacent upslope area where the most pronounced BSRs have been found (Figure 2).

Tectonic position and structural relationships largely define sediment types of the continental slope within the Nankai Trough study region. Subduction along this area probably started as recently as 3 to 5 m.y. ago (Moore and Karig, 1976) and continued intermittently to the present. As a result of the subduction processes, a series of ridges emerged on the slope. These ridges are the topographic expressions of thrust faults rooted in the basal detachment beneath the middle and upper slope. The ridges dammed downslope sediment transport forming sediment ponds or intraslope basins. While the sediment ponds differ with respect to the amounts of sediment contained (Hilde et al., 1969), accumulations generally increase in thickness upslope as the spacing between ridges increases. The presence of ridges and ponds has affected sedimentation in lower parts of the slope. The principal effect is the trapping of the mainly terrigenous sediments transported down the slope. With continuous sediment supply interrupted by the ridges, major turbidite sedimentation dominated in the axial zone of the trough. Thus, finer terrigenous sediments are expected in the upper sections of the lower slope where BSRs abound. Accreted hemipelagic muds and biogenic sediments are also to be expected in the upper slope. The rapid sedimentation probably increases quite dramatically the potential of the area with regard to bio-methanogenesis. Detailed assessment of the sediments in view of their hydrocarbon generation potential must await more direct data from the upslope areas.

Importance of reservoir characteristics in the processes of gas hydrate formation has been indicated by many authors (e.g. Makogon, 1978; MacLeod, 1982; Krason and Ridley, 1985). Although the quantitative relationship between grain size and gas hydrate formation is not known at the present time, the investigations carried out in this field at the Lubkin Petrochemical and Gas Industry Institute in Moscow provided some findings of a qualitative nature. It has been reported that lower temperatures and higher pressures are required for gas hydrate formation in porous medium compared with a free gas-water contact. This is primarily due to changes in water vapor pressure (Makogon, 1978). With smaller diameter of rock grains (i.e. smaller capillary radium) the depression of water vapor pressure is greater and consequently more stringent thermal and pressure conditions are needed for initiation of gas hydrate formation in porous environments.

In the Nankai Trough region high porosities and permeabilities can be expected particularly in the turbidite zones. The reservoir qualities of sediments in these areas may facilitate gas hydrate formations providing that pore water highly saturated in hydrocarbons is in abundance.

The role of sedimentation rates and erosional processes in gas hydrate formation has been discussed in detail by Krason and Ridley (1985). The high sedimentation rates of the Nankai Trough study region favor methane generation and thus gas hydrate formation. These rates (300-1340 m/m.y.) are sufficiently high to assure chemically reducing environment necessary for biomethanogenesis. Also, high deposition rates may have a modifying role on geothermal gradients.

Lithology can affect geothermal gradients. Although this factor plays a minor role in the Nankai Trough, typically increased thermal conductivity can be observed in strata with higher sand:shale ratio (MacLeod, 1982) which means that lower geothermal gradients can be anticipated in such areas.

Heat Flow

Geothermal conditions of an area control the subbottom depth of the gas hydrate stability zone in natural geologic environments. In the Nankai Trough study region, diverse and unusually high heat flows were consistently reported by a number of investigators (Yamano et al., 1982; Kinoshita and Yamano, 1986).

The first comprehensive regional study of the heat flow of the Nankai Trough study region was presented by Yamano et al. (1982), and based on wide occurrence of bottom simulating reflectors (BSRs) in the area. In order to calculate heat flow, two factors must be known: geothermal gradient and thermal conductivity of sediments. Assuming that BSRs represent the lower boundary of the gas hydrate stability zone, geothermal gradient values were derived from phase diagram for gas hydrates (Figure 19) and oceanographic observations of ocean floor temperatures. Thermal conductivity of sediments in the Nankai Trough was estimated from the relationship between compressional seismic wave velocity and thermal conductivity of marine sediments shown by Horai (1982). Although it had been shown experimentally that gas hydrate formation increases the velocity of compressional waves and decreases thermal conductivity of sediments (Stoll and Bryan, 1979), only marginal changes to these properties were observed in the Nankai Trough. These minor changes of the physical properties of the sediments in the Nankai Trough can probably be explained by the relatively thin hydrate zone (Shipley and Didyk, 1982). Thermal conductivity was estimated at 12 locations along multichannel seismic lines K-54-1-2, N55-3-1 and N 55-1 (Figure 20). In all cases a compressional wave velocity of $1.85 \pm .05$ km/sec and a sediment density of 1.9 g/cm^3 were used to estimate the thermal conductivity from Horai's (1982) curves. The best fit of the data from Nankai Trough was obtained with the thermal conductivity 2.9 ± 0.5 mcal cm sec °C. Direct measurements of the thermal conductivity of sediments at DSDP Site 298 (Figure 1) showed slightly lower values of 2.6 mcal cm sec °C (Karig et al., 1975). Results of the heat flow investigation in Nankai Trough are shown in Table 11 and Figures 21 and 22.

Conventionally obtained values of the heat flow (Watanabe et al., 1970; Soinov et al., 1972; Anderson et al., 1978) in the Nankai Trough are also plotted in Figure 22. Heat flow data shown in this figure revealed a surprisingly consistent pattern in the region. The highest values, above 2 HFU, have been observed in the area of the floor of the trough. Lower values, 1-2 HFU, were found in the continental slope.

One of the most recent direct measurements of temperature in sediments of the Nankai Trough was performed during DSDP Leg 87. In the topmost sediment layers, a temperature measuring device was installed in the cutting shoe of the hydraulic piston cover (HPC). The measuring procedure with this device has been described by Kagami et al. (1986). The other temperature probe was operated in combination with a Barnes water sampler (Yakota et al., 1980). Horai (1984)

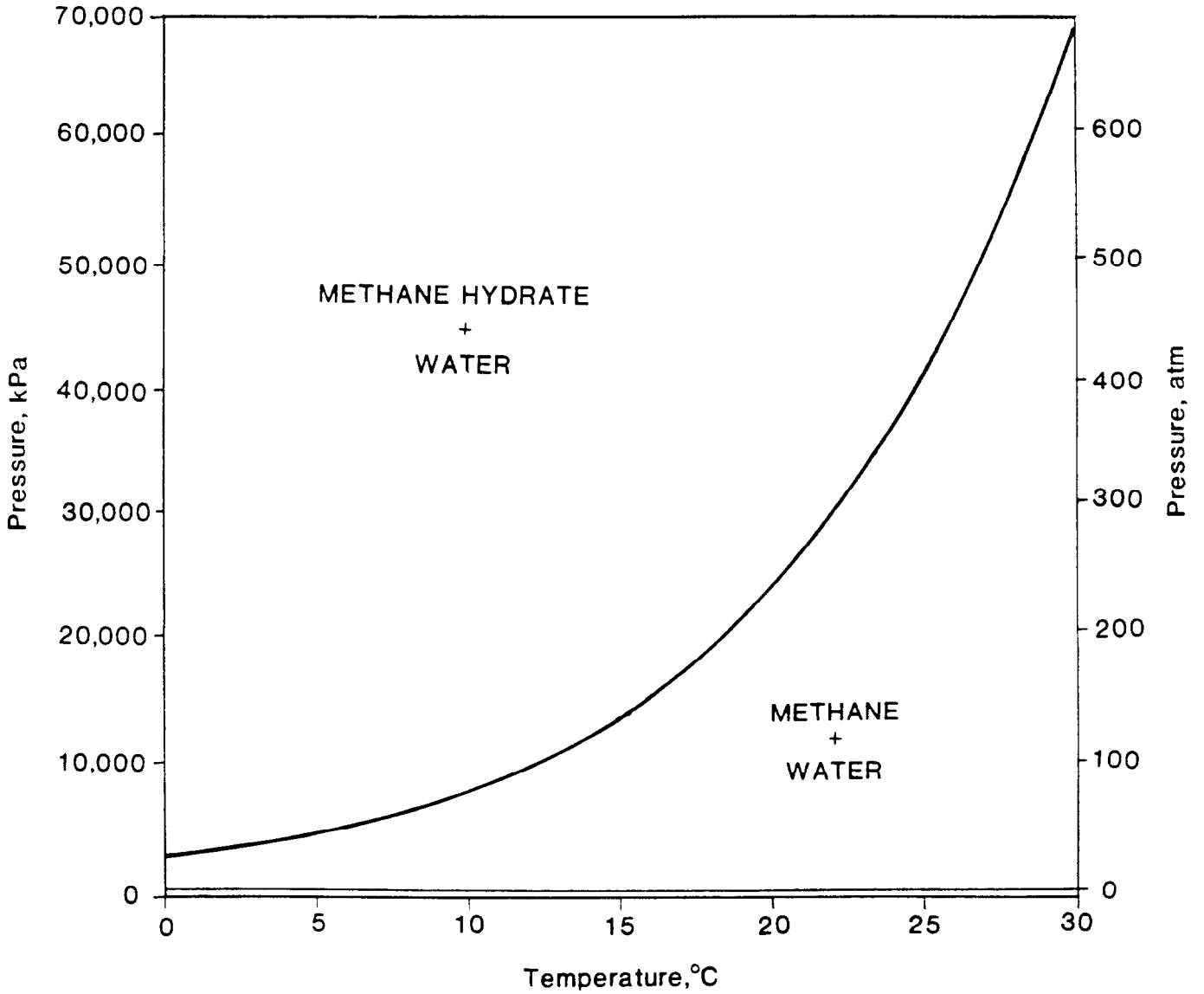

Figure 19. PHASE DIAGRAM OF METHANE AND WATER SYSTEM

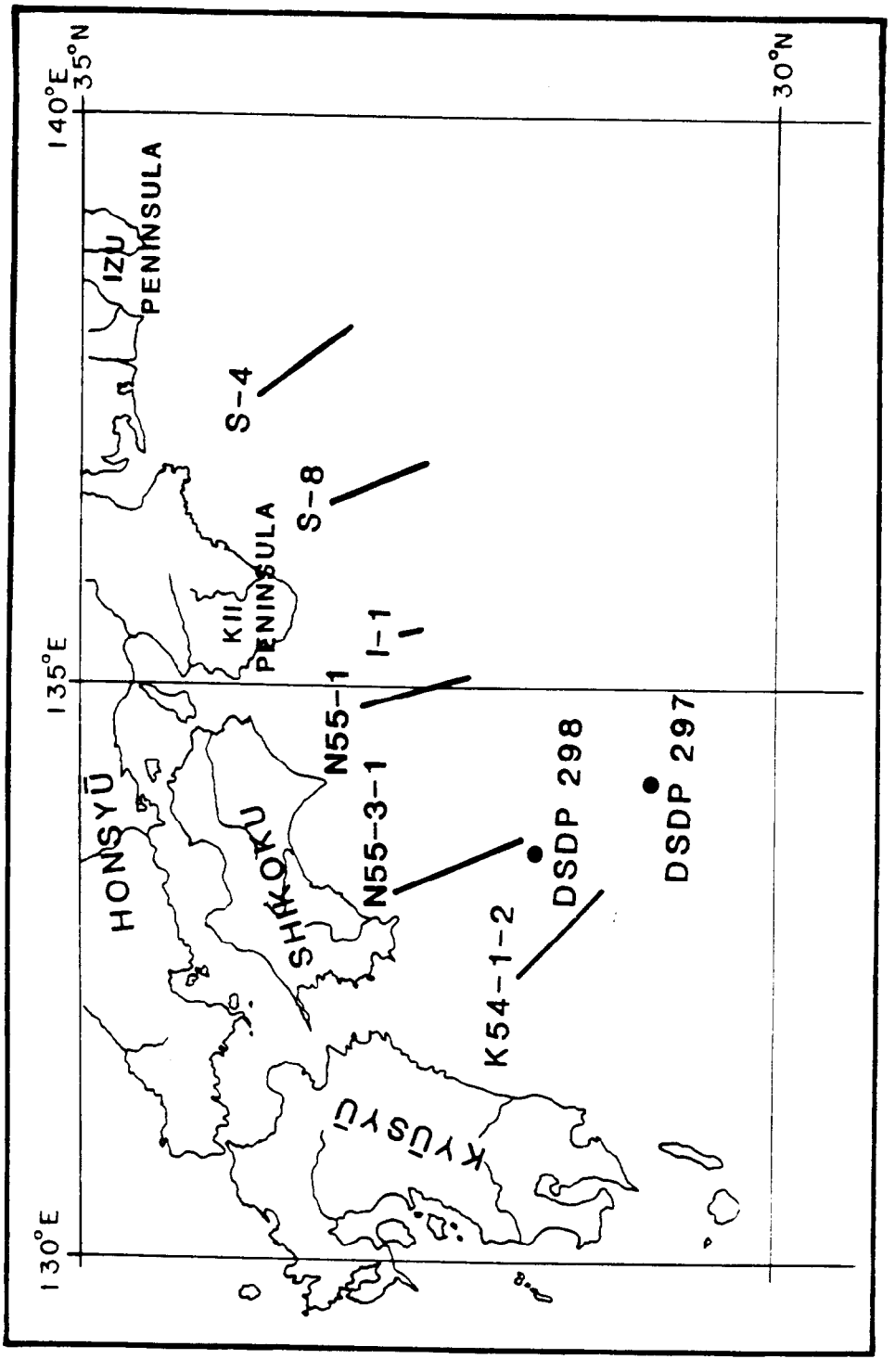

Figure 20. **LOCATION OF SEISMIC LINES IN THE STUDY REGION**

After Aoki et al., 1982

TABLE 11.

ESTIMATED HEAT FLOW AND GEOTHERMAL GRADIENTS IN NANKAI TROUGH

After Yamano et al., 1982

Site	Water Depth (m)	Gas Hydrate Phase Boundary					
		Depth (m)	Pressure (atm)	Temp. (°C)	Gradient (°C/km)	Heat Flow (HFU)	Heat Flow (mW/m^2)
1	2535	465	331	20.9	41.5	1.20	50
2	2685	445	343	21.2	44.0	1.28	54
3	2895	390	355	21.4	50.8	1.47	62
4	2880	415	357	21.5	48.0	1.39	58
5	2880	435	361	21.6	46.0	1.33	56
6	3040	350	363	21.7	57.7	1.67	70
7	2940	415	363	21.7	48.4	1.40	59
8	3320	340	389	22.1	60.6	1.76	74
9	3360	350	395	22.3	59.4	1.72	72
10	3370	390	402	22.4	53.6	1.55	65
11	3700	325	424	22.9	65.8	1.91	80
12	3850	380	448	23.4	57.6	1.67	70

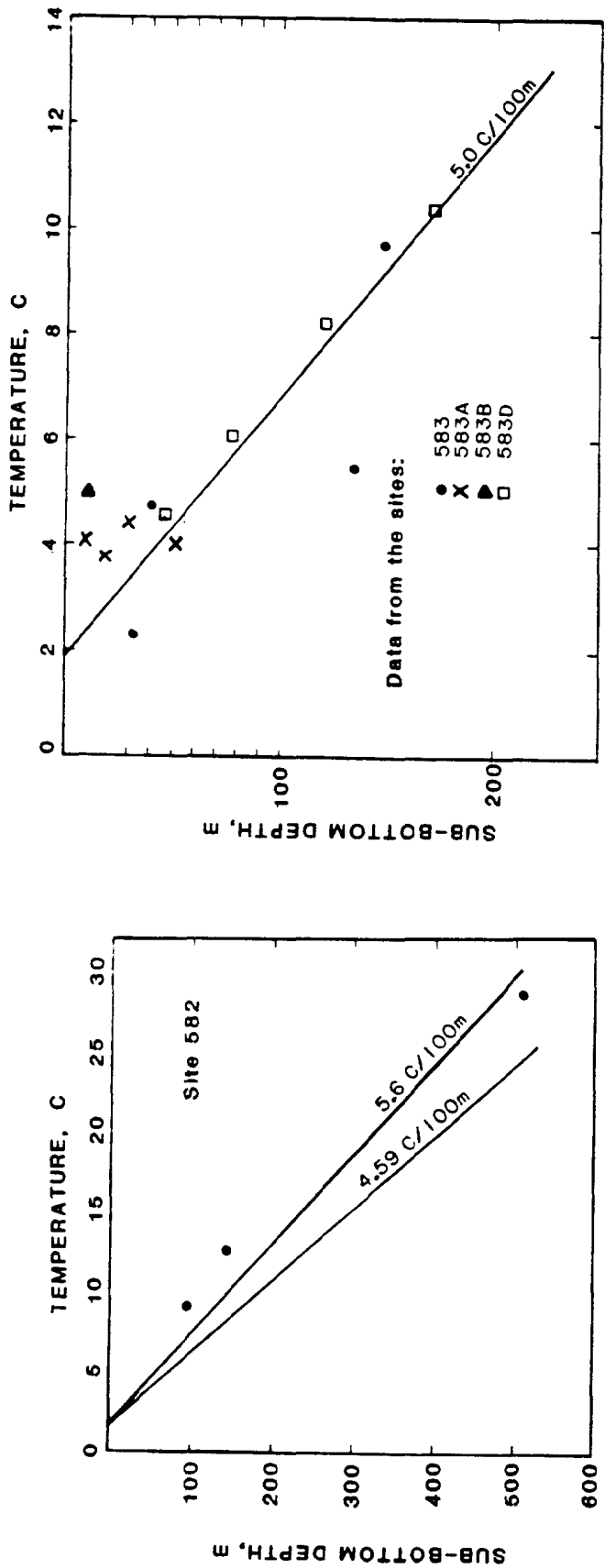

Figure 21. **SEDIMENT TEMPERATURES AND GEOTHERMAL GRADIENTS AT DSDP SITES 582 AND 583**
After Kagami et al., 1986

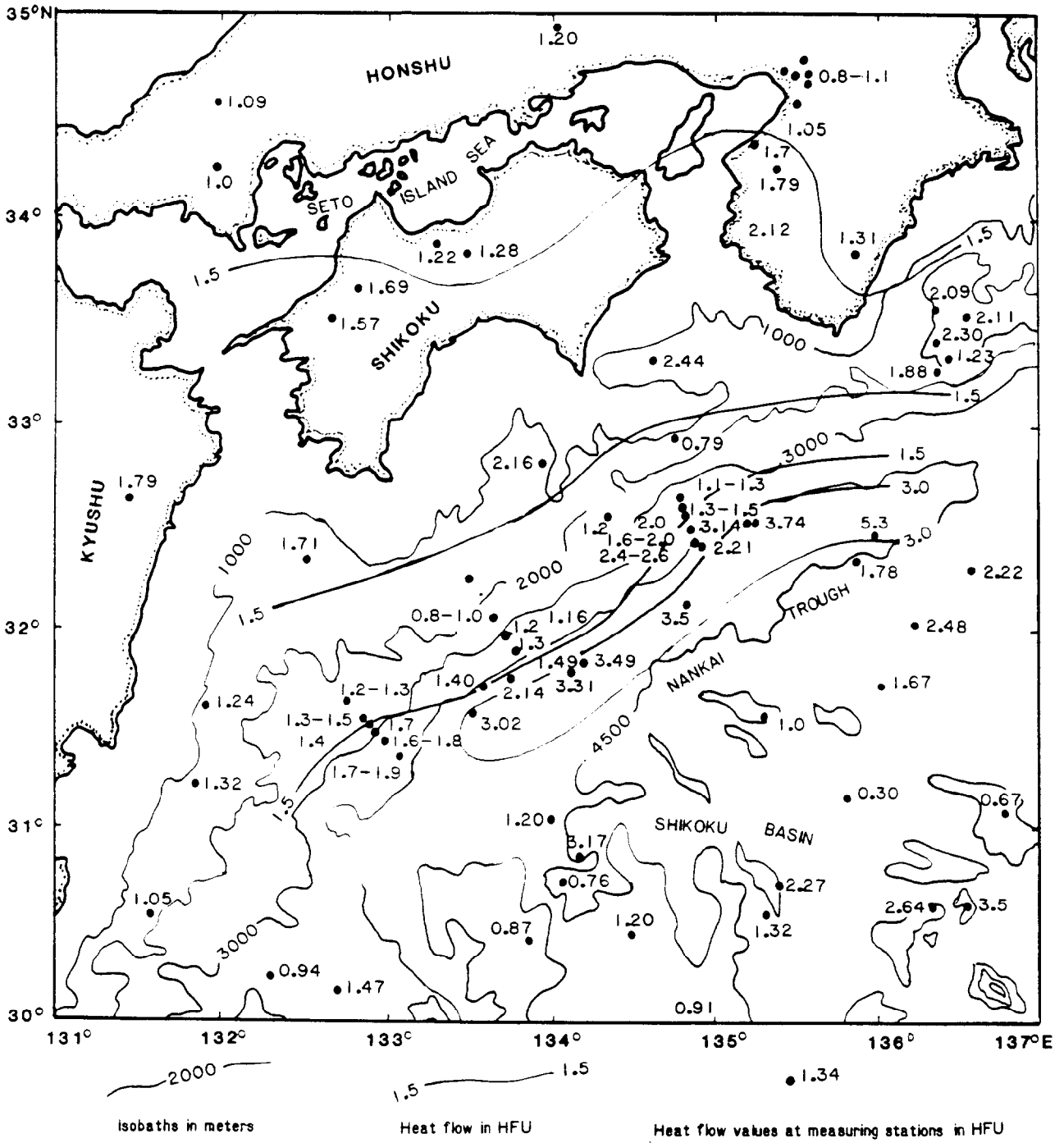

Figure 22. **MEASURED HEAT FLOW IN THE NANKAI TROUGH STUDY REGION.**

After Kagami et al., 1986

showed that the temperature measurements with probes during DSDP Leg 87 are reliable and accuracy of ±6% was obtained whenever a steady penetration of the probe was achieved. Thermal conductivities of the sediments were measured on every undisturbed core and averaged.

The geothermal data obtained from DSDP measurements was consistent with all previously obtained results showing high heat values in the Nankai Trough. More recent thermal measurements in the sediments of the Nankai Trough carried by scientists from the University of Tokyo with multiple penetration POGO apparatus (Hyndman et al., 1979) further corroborated the anomalous heat flow pattern in the area.

Explanations of conspicuously high heat flow in the Nankai Trough vary. Such heat flow values have not been identified in other trenches. The case of Nankai Trough may reflect the geothermal conditions of the Philippine Sea Plate. In view of the highly scattered heat flow (20-150 mW/m^2) within the Philippine Sea Plate, high values in the Nankai Trough are not excessive. On the other hand, well defined high heat flow zone in the trough is larger than anomalous areas within the Philippine Sea Plate. Kinoshita and Yamano (1986) suggested that three factors cause such high heat flux in the Nankai Trough:

- hot subducting plate
- migration of a hot fluid through structural pathway
- chemical reactions in the deep-sea sediments

The contention of an unusually hot subduction plate is based on the presence of several active and remnant spreading ridge systems on the Philippine Sea Plate. Also off-ridge volcanism and a number of small-scale lava intrusions into the sediments were suggested to have taken place about 13-15 m.y. ago (Klein et al., 1978). A deep origin of the heat flow anomaly in the Nankai Trough is further supported by a coincidence of the heat flow anomaly with other geophysical anomalies, including the conductivity anomaly of central Japan (Rikitake, 1966; 1969) and a residual gravity anomaly.

Kinoshita and Yamano (1986) suggested that hydrologic circulation may be responsible for producing high heat flow in the Nankai Trough. Although the entire process is not completely explained, the authors propose that water circulation occurs in the form of hot-spring upwelling. Interstitial water is warmed as it descends along the flanks of the shelf into the crust. The hot, buoyant water percolates through fault planes in the vicinity of the trough, thereby increasing regional heat flow.

The role of chemical reactions in sediments is probably minor. Kinoshita and Yamano (1986) described heat contributing processes which originate during decomposition and oxidation of organic matter beneath the ocean floor.

Sedimentation Rates

At least two aspects of sedimentation rates can be directly related to the processes of gas hydrate formation and their stability in geological environments. The first aspect is linked to bio-methanogenesis. Particularly in shallower marine

environments, reducing geochemical conditions necessary for organic matter biodegradation are best maintained when a sufficiently high rate of sedimentation takes place. The threshold sedimentation rate of 500 m/m.y. is considered sufficient to secure a reducing environment. The second aspect pertains to geothermal processes in sediments. As was extensively discussed by Krason and Ridley (1985), when sedimentation rates are less than 100 m/m.y., a steady-state gradient in newly deposited layers is achieved almost simultaneously with the deposition. On the other hand, higher sedimentation rates initially depress geothermal gradients producing a series of transient, lower geothermal gradients.

The rates at which sediments were deposited at the DSDP Site 582 are shown in Figure 23. During the last 1 m.y. the area is characterized by extremely high deposition rate varying from 300 to 1340 m/m.y. These high rates of sedimentation in the Nankai Trough contribute to gas hydrate formation.

Seismic Evidence for Gas Hydrates

At the present time seismic data constitute the principal evidence for gas hydrates in sediments of the Nankai Trough.

Seismic data are commonly used for identification of gas hydrates in marine sediments. The anomalous seismic reflectors referred to as bottom simulating reflectors (BSRs), which are frequently observed on seismic records from continental slopes and rises, are interpreted by many authors as the base of the gas hydrate-bearing zone (Stoll et al., 1971; Ewing and Hollister, 1972; Dillon et al., 1980; Shipley et al., 1979; and others). Since BSRs generally coincide approximately with isothermal surfaces, they max intersect reflections from sedimentary strata and generally mimic the topography of the sea floor. During the past several years efforts have been made toward better understanding the nature of the anomalous seismic responses from sediments in gas hydrate bearing zones as well as from the free gas zones underlying them. The investigations of temperature and pressure conditions in zones with BSRs, invariably show their coincidence with a gas hydrate thermodynamic stability field (Tucholke, 1977). Further evidence on the relationship between BSRs and gas hydrates was drawn from the investigations of seismic velocities in sediments where BSRs were previously identified. Lancelot and Ewing (1972) determined an apparent acoustic velocity of 2 km/sec through sediments overlying the BSRs. The assertions of Lancelot and Ewing (1972) were corroborated independently by Bryan (1974). Bryan found acoustic velocities in the gas hydrate zones which were excessively high for hemipelagic sediments.

In addition to the correspondence of BSRs and temperature and pressure stability conditions of hydrates, Bryan (1974) and Shipley et al. (1979) distinguished three additional criteria for gas hydrate-related BSRs:

1. reflection polarity reversal
2. large reflection coefficient, and
3. increased subbottom depth of the BSRs with increasing water depth

The concentration of free gas below gas hydrate zone decreases formation density and acoustic velocities. Thus the boundary between the gas hydrate zone and the underlying zone with gas should result in seismic polarity reversal and

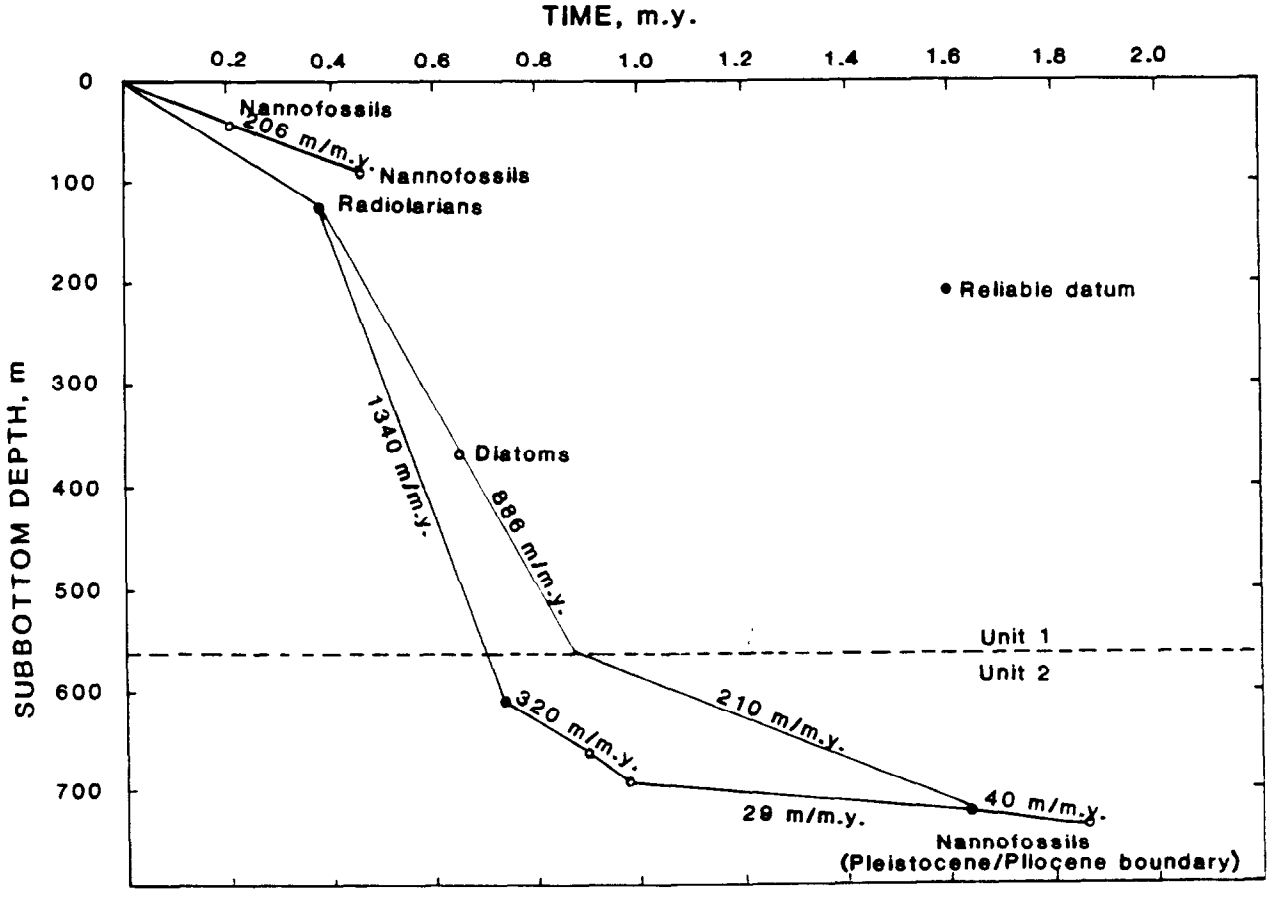

Figure 23. **SEDIMENTATION RATES AT DSDP SITE 582**
After Kagami et al., 1986

negative reflection coefficient. The seismic reflection coefficient (R) has been proposed as a measure of the acoustic velocity and formation density changes. The reflection coefficient was defined as:

$$R = (\rho_2 V_2 - \rho_1 V_1)/(\rho_2 V_2 + \rho_1 V_1)$$

where:

ρ_2, ρ_1 = formation density in gas hydrate zone and in free gas zone

V_2, V_1 = acoustic velocities in gas hydrate zone and in free gas zone

The relationship between water depth and subbottom depth of a BSR is considered as an important indicator of gas hydrate. If the BSRs represent the base of gas hydrate zone in the areas of uniform heat flow, the subbottom depth of their occurrence should increase with increasing sea water depth due to higher pressure conditions. This relationship is not always found within areas with anomalous seismic reflectors. Such BSRs can represent other than gas hydrate base boundary, for example diagenetic zones (Hein et al., 1979; Krason and Ciesnik, 1987). The analysis of BSRs in various parts of the continental margin of North and Central America by Shipley et al. (1979) showed that at ocean depths below 2,000 m the magnitude changes of gas hydrate stability zone thickness due to variations in water column thickness are significantly smaller compared with the shallower areas.

Seismic recordings from the Nankai Trough in the public domain feature BSRs most likely related to gas hydrates (Figure 24). Migrated seismic lines 54K-1-2, 55N-1, and 55N-3-1 (Figures 2, 25, 26) obtained by Japan Petroleum Exploration (JAPEX) from the ship Kaiyo Maru show very well developed BSRs. Despite the fact that structural features are obscure in many sections, distinct and mostly continuous BSRs occur in lower sections of the continental slope.

Line K54-1-2 (Figure 25) is located about 70 km southwest of DSDP hole 298 and runs perpendicular to the axis of the Nankai Trough (Figures 1 and 20). With the exception of lowermost inner slope a conspicuous BSR occurs almost continuously upslope to the major ridge at point C (Figure 1). The bottom simulating reflector mimics quite precisely the topography of the sea floor at subbottom depth ranging 314 to 425 m. The sea water depths vary in this area from 2,345 m to 3,780 m. The presumed gas hydrate zone appears to be located within temperature-pressure stability field for methane hydrate.

Seismic records show reversed polarity of BSRs. However, the bottom simulating reflectors do not increase in subbottom depth with increasing sea depths. This uncommon feature, however, can be perhaps explained by unusual geothermal conditions in the area.

Line 55N-3-1 (Figure 26) also runs perpendicular to the Nankai Trough approximately 100 km north. DSDP Sites 582 and 583 are located in the southern section of this direction from the previous line. A very pronounced and almost continuous BSR can be observed along the profile. The subbottom depth of the BSR varies from 272 m to 552 m with sea water depth 840 m to 3,780 m. Again the position of the lower boundary of the hydrate zone appears to be strongly controlled by the heat flow pattern in the area (Figure 20).

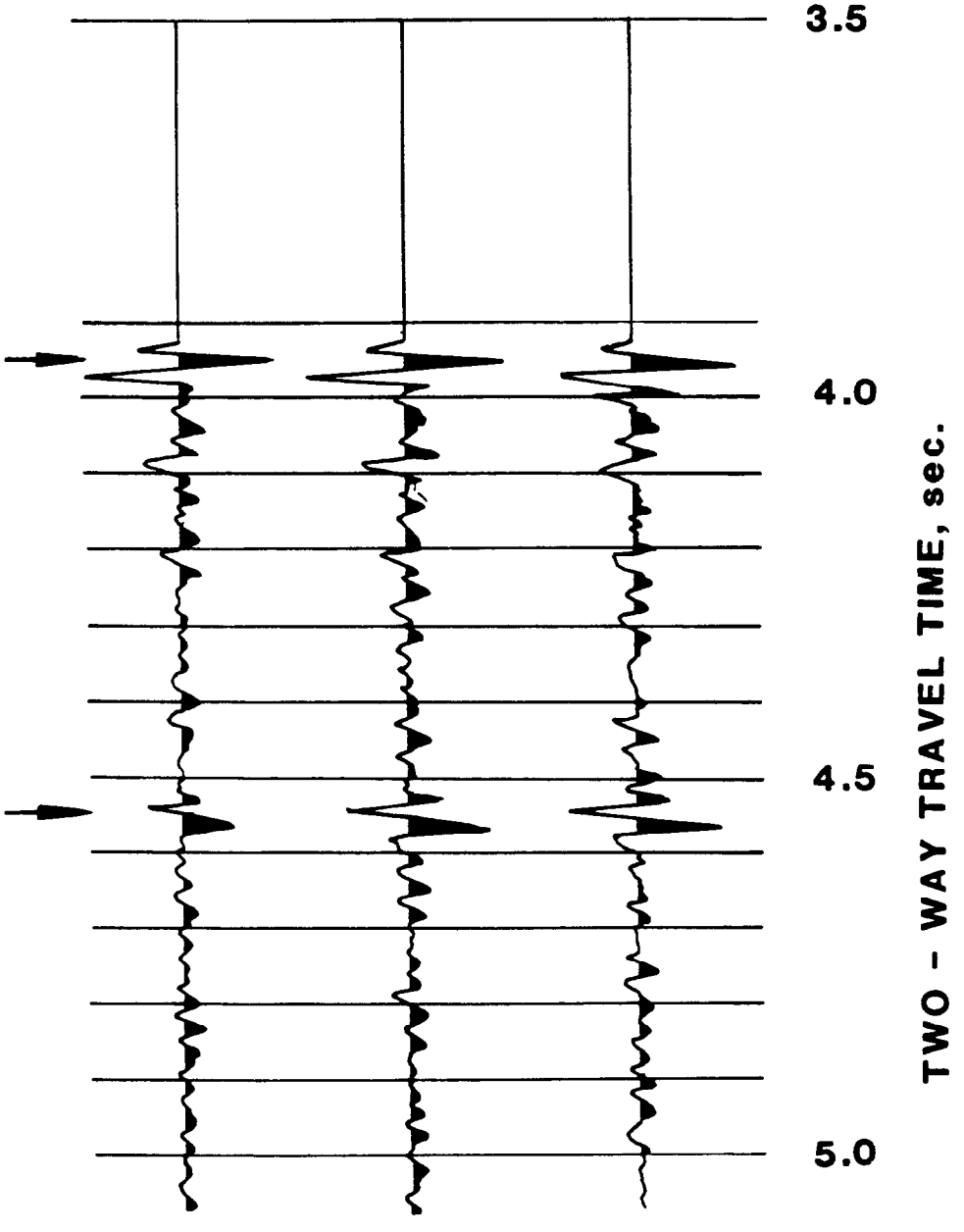

Figure 24. **INDIVIDUAL SHOT POINT TRACES FROM SEISMIC LINE 55-3-1 SHOWING REVERSE POLARITY OF BSR AT 4.55 sec.**
After Yamano and Uyeda, 1982

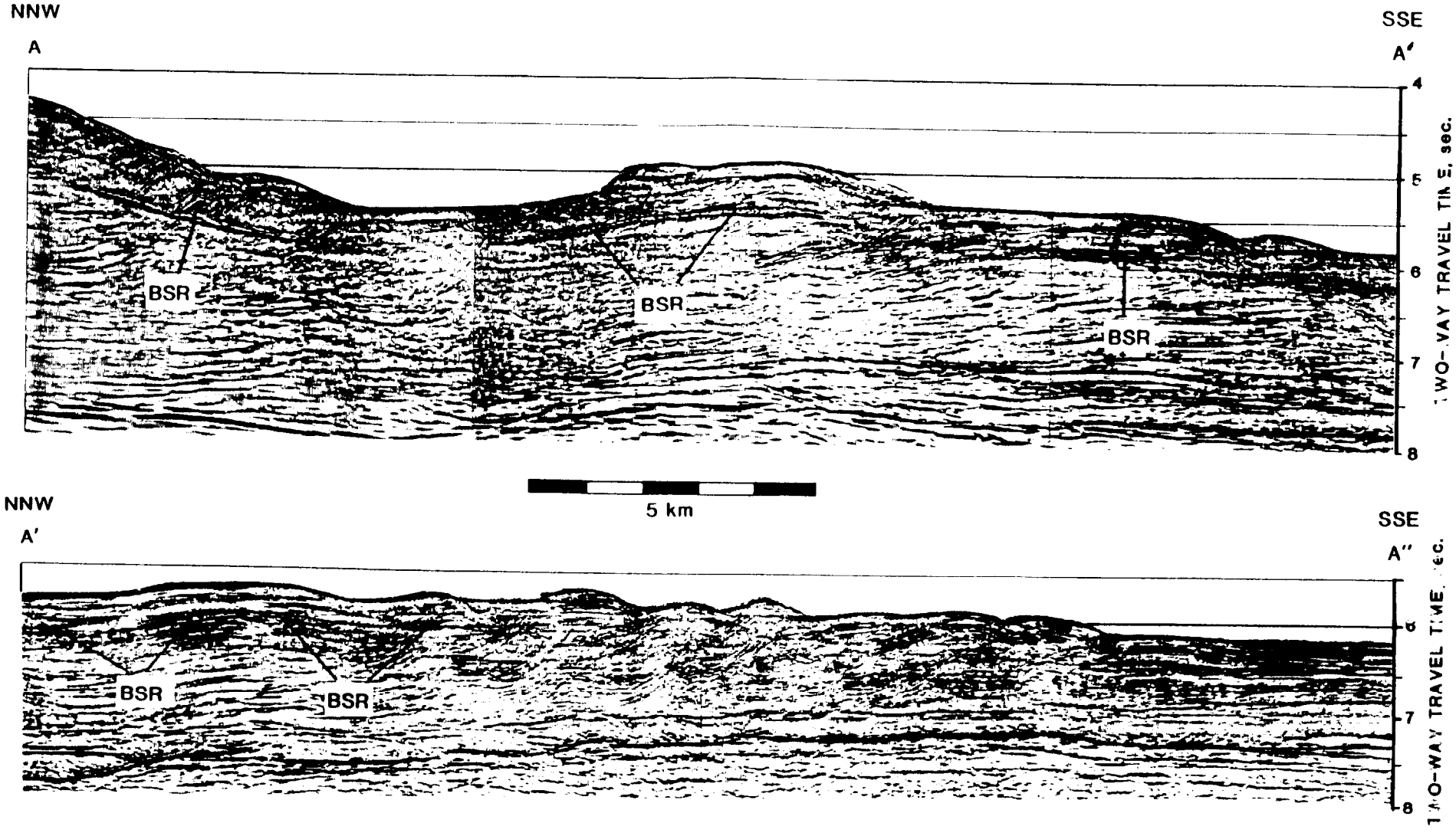

Figure 25. **SECTION OF SEISMIC LINE N55-1**

After Nasu et al., 1982

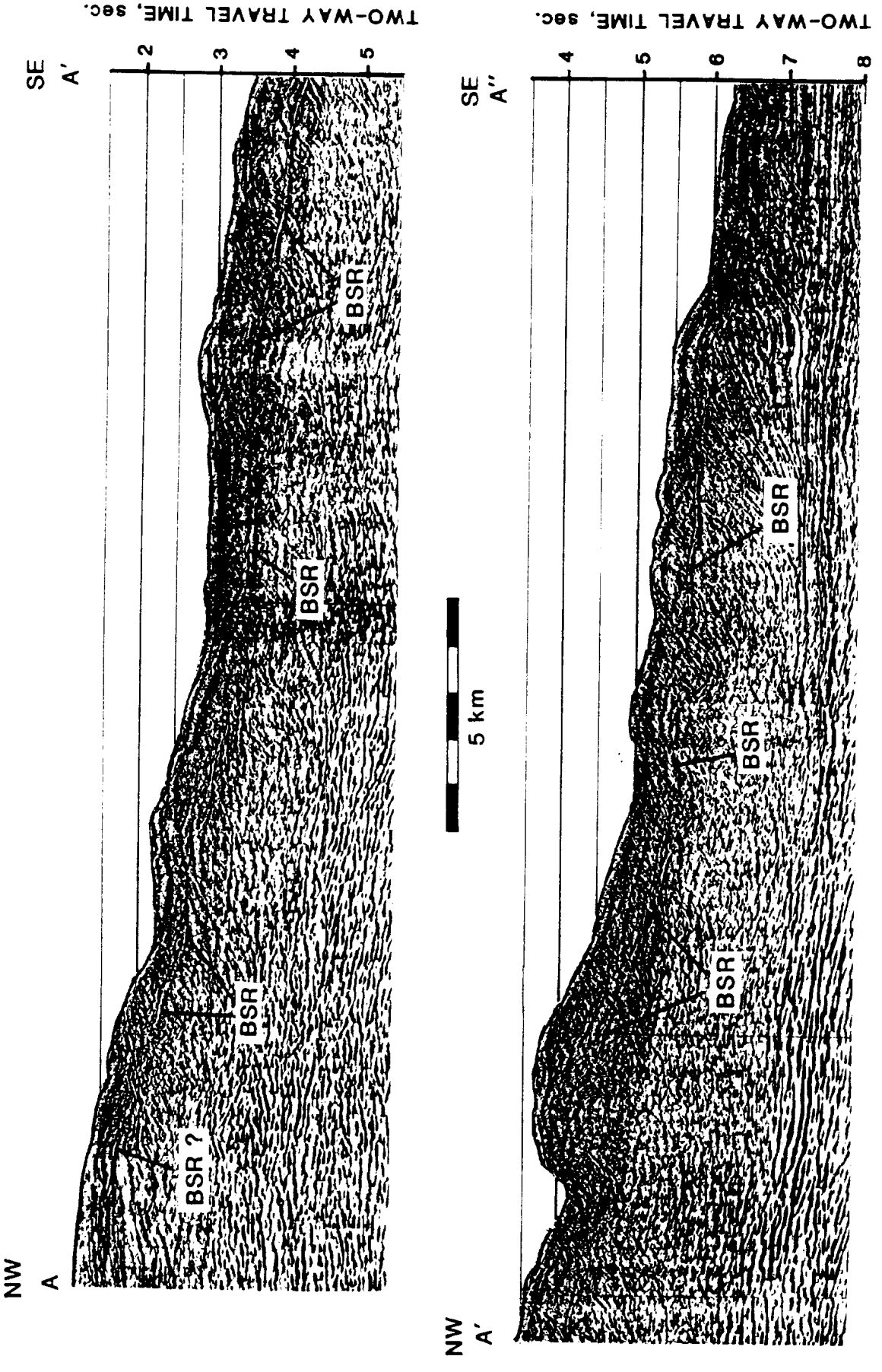

Figure 26. SECTION OF SEISMIC LINE N55-3-1

After Nasu et al., 1982

Line N55-1 (Figure 23) is the easternmost available seismic recording with noticeable BSRs in the Nankai Trough. The line includes areas from the trough floor through imbricated sediment wedges to pronounced major ridges produced by thrust faults. Although the most conspicuous BSRs are present within non-accreted sediments of the upper part of shown slope, the gas hydrate related reflectors can be traced to the lower slope areas. The subbottom depths of the BSRs vary from 255 m to 510 m between water depths of 3,290 and 4,095 m.

Direct Evidence of Gas Hydrates

The location of DSDP Site 583 on the major thrust fault in the Nankai Trough was partially motivated by the prospect of encountering gas hydrates, as a fault was thought to be a conduit to thermogenic gases. Carefully monitored drilling did not reveal the presence of gas hydrates, and Claypool et al. (1986) wrote, "There is no evidence for the presence of gas hydrates in these Leg 87 sediments." These observations were generally confirmed by lack of low salinity pore water (Hesse and Harrison, 1981), low concentration of organic matter and absence of methane generation below 30 m of subbottom depth as well as lack of BSRs on seismic recordings in the immediate vicinity of DSDP Site 583. Some doubts, however, as to the total absence of gas hydrates in sediments of DSDP Site 583 were expressed by Stein and Smith (1986). These authors described authigenic carbonate nodules recovered in the uppermost 50 m of the sedimentary sequence at Site 583. The crystals in the nodules from freshly recovered and split cores were described as "to be melting, changing luster and color to an opaque milky yellow in a matter of minutes." The reexamination of these cores approximately 6 months later revealed that crystalline aggregates disappeared entirely, "leaving only their molds and friable masses of pale yellow sand-size fragments." As a result of a number of mineralogical analyses, it has been concluded that the white nodules were crystals of the mineral ikaite which is a low temperature hydrated calcium carbonate ($CaCO_3$ $6H_2O$; Pauly, 1963). Stein and Smith (1986) stated that organic carbon supply sufficient for bio-methanogenesis, high sedimentation rates, high alkalinity and reducing conditions, jointly with sufficiently low temperatures, could have been extremely favorable for the precipitation of ikaite ($CaCO_3$ $6H_2O$) with possible clathrate ingredient (CH_4-$6H_2O$). As the precipitation of ikaite requires more stringent thermal condition, it is conceivable that crystalline aggregates of ikaite could have been stabilized by gas hydrates.

Certainly, solving the problem of ikaite aggregates and gas hydrates (?) discovered at Site 583 will require more direct analytical data from drill holes located perhaps in upslope areas of the Nankai Trough.

Assessment of Gas Resources in Gas Hydrates

Although gas hydrates have not been directly confirmed in the Nankai Trough, there are strong indirect features suggesting presence of a hydrate zone in this region. The analysis of various geological factors of the Nankai Trough revealed particular significance of geothermal processes as a major factor

controlling the areal extent of the hydrate zone. Temperature and pressure favorable for gas hydrate formation exist in most of the region. The full assessment of the gas hydrates must await more sedimentological and geochemical data from the inner (upslope) areas of the trough.

Based on the reviewed data from DSDP holes 582 and 583, there is reason to believe that hydrocarbons necessary in the process of gas hydrates in the upslope areas are most likely of biogenic origin. Perhaps greater supply of organic matter in these areas is related to upwelling processes which measurably increase biogenic production.

We estimate an areal extent of 3.5×10^{10} m^2 for the probable gas hydrate-bearing zone in the Nankai Trough region. Assuming 40% sediment porosity and 12% pore space filling, 5% of the sediment volume will be filled with gas hydrates. Using the 160:1 gas volume conversion factor from gas hydrates for standard conditions, the gas resource in the hydrate state (with the assumption of 40% areal extent) for the hydrate zone should amount to:

1 m thickness x 3.5×10^{10} m^2 area x 5% hydrate
x 40% areal extent x 160 volume conversion factor =
1.1×10^{11} m^3 (4 TCF)

For various mean thicknesses of hydrate layers, possible gas resources in gas hydrates are:

1 m = 1.1×10^{11} m^3 (4 TCF)
100 m = 110×10^{11} m^3 (400 TCF)
200 m = 220×10^{11} m^3 (800 TCF)
300 m = 330×10^{11} m^3 (1200 TCF)
400 m = 440×10^{11} m^3 (1600 TCF)

CONCLUSIONS

The Nankai Trough is one of 24 worldwide localities with strong indications of gas hydrate presence. Bottom simulating reflectors have been found solely in upslope areas north of the Nankai Trough (Figure 1). The total area with pronounced gas hydrate-related bottom simulating reflectors (BSRs) was found to be approximately 35,000 km^2. As no direct data from drilled holes are presently available, significant gaps still exist in fields of sedimentation, structural development of the region, thermal features and hydrocarbon generation. Based on existing seismic recordings and data from DSDP sites 297, 298, 582 and 583, some important conclusions relevant to gas hydrates were made:

1. Nankai Trough is a tectonically young active margin. The convergence rate between the Philippine Sea plate and Japanese Islands has been estimated at between 2 and 6 cm/y (Seno, 1977).

2. The structural features of the continental slope north of the Nankai Trough are well defined only in its lowermost part where imbricate sediment wedges are rather easily discernible. A system of ridges parallel to the trough axis constitutes another major structural feature of the region significantly controlling the sedimentation patterns.

3. DSDP cores from the lowermost accretionary wedges revealed the presence of accreted hemipelagic sediments from the Shikoku Basin and turbidites from the central Honshu Island transported along the trench's axis, and to a lesser degree slumped from upslope area sediments.

4. Rates of sedimentation in the entire region have been conspicuously high from the Pleistocene ranging from 300 to 1,340 m/m.y. It constitutes a favorable factor for biogenic hydrocarbon generation as well as in depressing geothermal gradients.

5. Analyses of hydrocarbon gases in sediments at the DSDP sites in the region unequivocally confirmed their biogenic origin.

6. The heat flow pattern in the Nankai Trough region is the most intriguing factor relevant to gas hydrate formation. While exceptionally high values of heat flow have been observed in the area of the Nankai Trough floor (over 2 HFU), depressed values were found in sediments of inner upslope areas (Figure 1). Lack of equilibrated geothermal conditions in the region are indicative of tectonically young areas (Anderson and Skilbeck, 1981).

7. Distinct bottom simulating reflectors appear on migrated seismic records from the upper sectors of the lower continental slope. Water depths in these sectors vary from 850 to 4,095 m whereas their subbottom depths range from 255 to 552 m. The subbottom depth figures are in good agreement with available lab experimental data.

8. The distribution of the BSRs correlates well with the regional heat flow pattern, which seems to be a major controlling factor for gas hydrate zones.

9. Production of in situ organic matter is perhaps greater in the upper sections of the continental slope as a result of processes associated with upwelling currents. Thus a greater supply of organic matter to the areas of biogenic hydrocarbon generation creates more favorable conditions for gas hydrate formation.

10. The estimated resources of hydrocarbon gas locked in the presumed hydrate zone per 1 m thickness of this zone in and adjacent to the Nankai Trough region is 1.1×10^{11} m^3 or 4 TCF. Assuming an average thickness of the hydrate zone in the area of 30 m, the total amount of gas in the zone would be 120 TCF.

REFERENCES

Anderson, R.N., Langseth, M.G., Hayes, D.H., Watanabe,T., and Yasui, M., 1978, Heat flow, thermal conductivity, thermal gradient, *in* E.D. Hayes ed., Geophysical atlas of the east and southeast Asian Seas: Geological Society of America map and Chart Series, MC-25.

Aoki, Y., Tamano, T., and Kato, S., 1982, Detailed structure of the Nankai Trough from migrated seismic sections, *in* J.S. Watkins and C.L. Drake eds., Studies in continental margins, AAPG Memoir 34, p. 309-322.

Bates, R.L., and Jackson, J.A., 1980, Glossary of Geology: Falls Church, Virginia, American Geological Institute, 2d ed., 751 p.

Bernard, B.B., Brooks, J.M., and Sackett, W.M., 1976, Natural gas seepage in the Gulf of Mexico: Earth and Planet. Sci. Lett., v. 31, p. 48-54.

Bryan, G.M., 1974, In situ indications of gas hydrates, *in* Kaplan, I.R., ed., Natural Gases in Marine Sediments: New York, Plenum Press, p. 299.

Claypool, G.E., Vuletich, A.K., and Kvenvolden, K.A., 1986, Isotopic composition of interstitial fluids in sediment of the Nankai Trough, Deep Sea Drilling Project, Leg 87, *in* Initial reports of the Deep Sea Drilling Project, Yokohama, Japan to Yokohama, Japan, v. 87: Washington, D.C. Government Printing Office, p. 857-860.

Dillon, W.P., Grow,J.A., and Paull, C.K., 1980, Unconventional gas hydrate seals may trap gas of southwest U.S.: Oil and Gas Jour., v. 78, no. 1, p. 124.

Dow, W.G., 1977, Kerogen studies and geological interpretations: Journal of Geochemical Exploration, v. 7, no. 1, p. 79-99.

Espitalie, J., Laporte, J.L., Madec, M., Marquis, F., Leplat, P., Paulet, J., and Boutefeu, A., 1977, Méthode rapide de caractérisation des roches mères, de leur potentiel pétrolier et de leur degré d'évolution: Revue de l'Institut Français du Pétrole, v. 32, p. 23-42.

Ewing, J.I., and Hollister, P., 1972, Regional aspects of deep sea drilling of the western North Atlantic, *in* Initial reports of Deep Sea Drilling Project, New Jersey, v. 11: Washington, U.S. Govt. Printing Office, p. 951-973.

Hein, J.R., Scholl, D.W., Barron, J.A., Jones, M.G., and Miller, J., 1978, Diagenesis of late Cenozoic diatomaceous deposits and formation of the bottom simulationg reflector in the southern Bering Sea: Sedimentology, v. 25, p. 155-181.

Hesse, R., and Harrison, W.E., 1981, Gas hydrates (clathrates) causing pore-water freshening and oxygen isotope fractionation in deep water sedimentary sections of terrigenous continental margins: Earth Planet. Sci. Letters, v. 55, p. 453-462.

Hilde, T.C., Wageman, J.M., and Hammond, W.T., 1969, The structure of Tosa terrace and Nankai Trough off southern Japan: Deep-Sea Research, v. 16, p. 67-76.

Hirahara, K., 1980, Three-dimentional P-wave velocity distribution in southwestern Japan: Annual Meeting of the Seismological Society of Japan, n. 2.

Horai, K., 1982, Thermal conductivity of sediments and igneous rocks recovered during DSDP Leg 60, *in* Initial reports of the Deep Sea Drilling Project, v. 60: Washington, D.C., Govt. Printing Office, p. 534-545.

Hunt, J.M., 1979, Petroleum geochemistry and geology: San Francisco, W.H. Freeman, 617 p.

Hyndman, R.D., Davis, E.E., and Wright, J.A., 1979, The measurement of marine geothermal heat flow by a multipenetration probe with digital acoustic telemetry and in situ thermal conductivity: Mar. Geophys. Research, v. 4, p. 181-205.

Kagami, H., Karig, D.E., Coulbourn, W.T., et al., 1986, Site 583, *in* Initial reports of the Deep Sea Drilling Project, Yokohama, Japan to Yokohama, Japan, Leg 87: Washington, D.C., Govt. Printing Office, p. 123-256.

Kanamori, H., 1972, Tectonic implications of the 1944 Tonkai and the 1946 Nankaido earthquakes: Physics of the Earth and Planetary Interiors, v. 5, p. 129-139.

Kaneko, S., 1966, Transcurrent displacement along the Median line, southwestern Japan: N.Z.J. Geol. Geophys., n. 1, p. 45-49.

Karig, D.E., et al., 1975, Site 298, *in* Initial reports of the Deep Sea Drilling Project, v. 31: Washington, D.C., Govt. Printing Office, p. 317-350.

Kinoshita,H., and Yamano, M., 1986, The heat flow anomaly in the Nankai Trough area, *in* Initial reports of the Deep Sea Drilling Project, Yokohama, Japan to Yokohama, Japan, Leg 87: Washington D.C., Govt. Printing Office, p. 737-742.

Klein, G. de V., Kobayashi, K., Chamley, H., Curtis, D.M., Dick, H.J.B., Echols, D.J., Fountain, D.M., Kinoshita, H., Marsh, N.G., Mizumo, A., Nisterenko, G.W., Okada, H., Sloan, J.R., Waples, D.M., and White, S.M., 1978, Off-ridge volcanism and sea floor spreading in the Shikoku Basin: Nature, n. 273, p. 746-748.

Krason, J., and Ciesnik, M.S., 1986, Gas hydrates in the Russian literature: U.S. Dept. of Energy, 154 p. (in press).

Krason, J., and Ciesnik, M.S., 1987, Basin analysis, formation and stability of gas hydrates in the Aleutian Trench and the Bering Sea: Geological evolution and analysis of confirmed or suspected gas hydrate localities, Volume 10: U.S. Department of Energy publication, DOE/MC/21181-1950, 10 (DE86006637J), 152 p.

Krason, J., and Ridley, W.I., 1985, Basin analysis, formation and stability of gas hydrates in the Blake-Bahama Outer Ridge, U.S. East Coast, in series of Geological evaluation and analysis of confirmed or suspected gas hydrate localities: U.S. Department of Energy, Office of Fossil Energy, Morgantown Energy Technology Center, v. 1, 100 p.

Kuuskraa, V.A., Hammershaimb, E.C., Holder, G.D., Sloan, E.D., 1983, Handbook of gas hydrate properties and occurrence: U.S. Department of Energy, DOE/MC/19239-1546, U.S. Govt. Printing Office, Washington, 234 p.

Kvenvolden, K.A., and Barnard, L.A., 1983, Hydrates of natural gas in continental margins, *in* Watkins, J.S., and Drake, C.L., eds., Studies in continental margin geology: Am. Assoc. Petroleum Geologists Mem. 34, p. 631-640.

Kvenvolden, K.A., and McMenamin, 1980, Hydrates of natural gas, a review of their geological occurrence: U.S. Geol. SurveyCirc. 825, 11 p.

Lancelot, Y., and Ewing, J.I., 1972, Correlation of natural gas zonation and carbonate diagenesis in Tertiary sediments from the northwest Atlantic, *in* Initial reports of Deep Sea Drilling Project, Miami, Florida to Hoboken, New Jersey: Washington, U.S. Govt. Printing Office, v. 11, p. 791.

Ludwig, W.J., Den, S., and Muranchi,S., 1973, Seismic reflection measurements of southwest Japan margin: Jour. Geophys. Research, v. 78, p. 2508-2516.

MacLeod, M.K., 1982, Gas hydrates in ocean bottom sediments: Am. Assoc. Petroleum Geologists Bull., v. 6, p. 2649-2662.

Makogon, Y.F., 1974, Gidrati prirodnykh gazov (Hydrates of natural gas): trans. by W.J. Cieslewicz, 19778, Geoexplorers Associates, Inc., Denver, 178 p.

Moore, J.C., and Karig, D.E., 1976, Sedimentology, structural geology and tectonics of the Shikoku subduction zone: Geological Society of America Bulletin, v. 87, p. 1259-1268.

Mukhopadhyay, P.K., Rulkötter, J., Schaefer, R.G., and Welte, D.H., 1986, Facies and diagenesis of organic matter in Nankai Trough sediments, Deep Sea Drilling Project, Leg 87A, *in* Initial Reports of the Deep Sea Drilling Project, Yokohama, Japan to Yokohama, Japan, v. 87: Washington, D.C., Govt. Printing Office, p. 877-890.

Niitsuma, N., and Akiba, F., 1986, Magneto-stratigraphy and diatom biostratigraphy of Site 587, Deep Sea Drilling Project, Leg 87, and implications for the tectonic evolution of Japanese island arcs, *in* Initial reports of the Deep Sea Drilling Project, Yokohama, Japan to Yokohama, Japan, v. 87, Washington, D.C., Govt. Printing Office, p. 555-572.

Ohtsuka, K., 1980, Results of piston-core sampling in Suruga Bay, central Japan during the research cruises KT-77-7 and KT-78-19 of R/V Tansei-Maru: Geosci. Rep. Shizuoka University, v. 5, p. 23-30.

Rikitake, T., 1966, Electromagnetism and the Earth's interior: Amsterdam, Elsevier, 60 p.

Rikitake, T., 1969, The undulation of an electrically conductive layer beneath the islands of Japan: Tectonophysics, v. 7, p. 257-264.

Rullkötter, J., Flekken, P., and Welte, D.H., 1980, Organic petrography and extractable hydrocarbons of sediments from the northern Philippine Sea, *in* Initial reports of the Deep Sea Drilling Project, Leg 58: Washington, D.C., Govt. Printing Office, v. 58, p. 755-762.

Sato, T., 1962, Sand and gravel bed cored from the bottom of the Surga Bay: Jour. Geol. Soc. of Japan, v. 68, p. 609-617.

Sekiguchi, K., and Hirai, A., 1986, Organic geochemistry of sediments from Deep Sea Drilling Project, Sites 582 and 583, Nankai Trough and Site 584, Japan Trench, *in* Initial reports of the Deep Sea Drilling Project, Yokohama, Japan to Yokohama, Japan, v. 87: Washington, D.C., Govt. Printing Office, p. 897-908.

Shipley, T.H., Houston, M.H., Buffler, R.T., Shaub, F.J., McMillen, K.J., Ladd, J.W., and Worzel, J.L., 1979, Seismic evidence for widespread possible gas hydrate horizons on continental slopes and rises: Am. Assoc. Petroleum Geologists Bull., v. 63, p. 2204-2213.

Shipley, T.H., and Didyk, B.M., 1982, Occurrence of methane hydrates offshore southern Mexico, *in* Watkins, J.S., Moore, J.C., et al., Initial reports of the

Deep Sea Drilling Project, v. 66: Washington, D.C., U.S. Govt. Printing Office, p. 547-556.

Soinov, V.V., Tikhomirov, V.M., Veserov, O.V., and Yeremin, G.D., 1972, Heat flow measurements during the Philippine Expedition of Sakhalin Complex Scientific Research Institute Transactions, v. 26, p. 212-215 (in Russian).

Stein, C.L., and Smith, A.J., 1986, Antigenic carbonate nodules in the Nankai Trough, Site 583, *in* Initial reports of the Deep Sea Drilling Project, Yokohama, Japan to Yokohama, Japan, leg 87: Washington, D.C., Govt. Printing Office, p. 659-668.

Stoll, R.D., and Bryan, G.M., 1979, Physical properties of sediments containing gas hydrates: Jour. Geophys. Research, v. 84, p. 1629.

Stoll, R.D., Ewing, J., and Bryan, G.M., 1971, Anomalous wave velocities in sediments containing gas hydrates: Jour. Geophys. Research, v. 76, p. 2090-2094.

Stoll, R.D., and Bryan, G.M., 1979, Physical properties of sediments containing gas hydrates: Jour. Geophys. Research, v. 84, p. 1629-1634.

Taira, A., and Niitsuma, N., 1986, Turbidite sedimentation in the Nankai Trough as interpreted from magnetic fabric, grain size, and detrital modal analyses, *in* Initial reports of the Deep Sea Drilling Project, Yokohama, Japan to Yokohama, Japan, v. 87, Washington, D.C., Govt. Printing Office, p. 611-632.

Tissot, B.P., Espitalié, B., and Combaz, A., 1974, Influence of nature and diagenesis of organic matter in formation of petroleum: Am. Assoc. Petroleum Geologists Bull., v. 58 (3), p. 499-506.

Tissot, B.P., and Welte, D.H., 1978, Petroleum formation and occurrence: Springer-Verlag, Berlin, 699 p.

Vassoevich, N.B., Korchagina, Yu.L., Lopatin, N.V., and Chernyshev, V.V., 1969, Principal phase of oil formation: Int. Geol. Rev., no. 12, p. 1276-1296.

Waples, D.W., and Sloan, J.R., 1980, Carbon and nitrogen profiles in deep-sea sediments; new evidence for bacterial diagenesis at great depths of burial: *in* Initial reports of the Deep Sea Drilling Project, Leg 58: Washington, D.C., Govt. Printing Office, v. 58, p. 745-754.

Watanabe et al., 1977, Heat flow in back-arc basins of the western Pacific, *in* M. Talwani, and W.C., Pittman, eds., Island arcs, Deep Sea Trenches and Back-Arc Basins: Washington, Maurice Ewing Series 1, American Geophysical Union, p. 137-161.

Watanabe, T., Epp, D., Uyeda, S., Langseth, M., and Yasui, M., 1970, Heat flow in the Philippine Sea: Tectonophysics, v. 10, p. 205-222.

Watanabe, T., Langseth, M.G., and Anderson, R.N., 1977, Heat flow in back-arc basins of the western Pacific: Am. Geophys. Union, Maurice Ewing Series 1, p. 137-161.

Yakota, T., Kinoshita, H., and Uyeda, S., 1980, New DSDP (Deep Sea Drilling Project) downhole temperature probe utilizing 1 C RAM (memory) elements: Bull. Earthquake Res. Inst. University of Tokyo, v. 55, p. 75-88.

Yamano, M., Uyeda, S., Hoki, Y., and Shipley, T.H., 1982, Estimates of heat flow derived from gas hydrates: Geology, v. 10, p. 339-343.

Yamazaki, F., Oida, T., and Aoki, H., 1980, Subduction of the Philippine plate in Tokai district: Seismological Society of Japan Annual Meeting, n. 2.